UNCLASSIFIED

LEVEL

ARL-STRUC-TECH-MEMO-300

AR-001-745

ADA086721

DEPARTMENT OF DEFENCE

DEFENCE SCIENCE AND TECHNOLOGY ORGANISATION

AERONAUTICAL RESEARCH LABORATORIES

MELBOURNE, VICTORIA

Structures Technical Memorandum 300

CALIBRATION OF MIRAGE MAIN UNDERCARRIAGE TO DETERMINE WHEEL LOADS FROM MEASURED STRAINS

K.C. WATTERS and P. ATCLIFFE

Approved for Public Release.

JULY, 1979

COPY No 7

UNCLASSIFIED

80 7 11 003

(12)

AR-001-745

DEPARTMENT OF DEFENCE

DEFENCE SCIENCE AND TECHNOLOGY ORGANISATION

AERONAUTICAL RESEARCH LABORATORIES

14 ARL/STRUC-TM-300

Structures Technical Memorandum 300

9

6 CALIBRATION OF MIRAGE MAIN UNDERCARRIAGE TO DETERMINE WHEEL LOADS FROM MEASURED STRAINS

10 K.C. WATTERS and P. RATCLIFFE

11 Jul 79

12 61

SUMMARY

The port and starboard legs of a test main undercarriage of the Mirage IIIO have each been instrumented with six independent strain gauges and a potentiometer to measure oleo deflection. Calibration tests were performed in which components of the ground-to-wheel load were applied to each leg, both singly and in combination, and, from the measured strains, calibration parameters were derived. In order to determine wheel load components from measured strains, an iterative method of inverting the non-linear set of equations formed from the calibration parameters was developed. It was found that, due to the insensitive response of any gauge to the vertical load component, the equations were ill-conditioned, with calculated load components being very sensitive to changes in the measured strains.

POSTAL ADDRESS: Chief Superintendent, Aeronautical Research Laboratories, Box 4331, P.O. Melbourne, Victoria, 3001, AUSTRALIA.

008 650

DOCUMENT CONTROL DATA SHEET

Security classification of this page: UNCLASSIFIED

1.	DOCUMENT NUMBERS	2.	SECURITY CLASSIFICATION
a.	AR Number: AR-001-745	a.	Complete document: UNCLASSIFIED
b.	Document Series and Number: Structures Technical Memorandum 300	b.	Title in isolation: UNCLASSIFIED
c.	Report Number: ARL-STRUC-TECH-MEMO-300	c.	Summary in isolation: UNCLASSIFIED

3. TITLE:

CALIBRATION OF MIRAGE MAIN UNDERCARRIAGE TO DETERMINE WHEEL LOADS FROM MEASURED STRAINS

4.	PERSONAL AUTHORS: K.C. WATTERS and P. ATCLIFFE	5.	DOCUMENT DATE: JULY, 1979
		6.	TYPE OF REPORT AND PERIOD COVERED:
7.	CORPORATE AUTHOR(S): Aeronautical Research Laboratories	8.	REFERENCE NUMBERS
		a.	Task: AIR 76/247
		b.	Sponsoring Agency: DEPT. OF DEFENCE (AIR FORCE OFFICE)
9.	COST CODE: 24 1235		
10.	IMPRINT: Aeronautical Research Laboratories, Melbourne	11.	COMPUTER PROGRAM(S) (Title(s) and language(s)): MIR3UC FORTRAN

12. RELEASE LIMITATIONS (of the document):

Approved for Public Release.

12-0. OVERSEAS:	N.O.		P.R.	1	A		B		C		D		E	

13. ANNOUNCEMENT LIMITATIONS (of the information on this page):

No Limitations.

14. DESCRIPTORS:	15. COSATI CODES:
Undercarriage. Mirage Aircraft.	0102
Takeoff	2011
Wheels	1402
Loads (Forces)	
Strain Gauges	
Calibrating	

16. ABSTRACT:

The port and starboard legs of a test main undercarriage of the Mirage IIIO have each been instrumented with six independent strain gauges and a potentiometer to measure oleo deflection. Calibration tests were performed in which components of the ground-to-wheel load were applied to each leg, both singly and in combination, and, from the measured strains, calibration parameters were derived. In order to determine wheel load components from measured strains, an iterative method of inverting the non-linear set of equations formed from the calibration parameters was developed. It was found that, due to the insensitive response of any gauge to the vertical load component, the equations were ill-conditioned, with calculated load components being very sensitive to changes in the measured strains.

CONTENTS

NOTATION

$\{\varepsilon\}$	vector of measured strains
$\varepsilon_{1 \text{ to } 6}$	components of $\{\varepsilon\}$ in microstrain
$\{F\}$	load vector
$F_{1 \text{ to } 6}$	components of $\{F\}$ in kgf or kgf.m
V	vertical load component in kgf and corresponds to F_1
D	drag load component in kgf and corresponds to F_2
S	side load component in kgf and corresponds to F_3
M_V, M_D, M_S	moments about V, D and S axes in kgf.m and correspond to F_4, F_5 and F_6 respectively
A	calibration matrix
a_{mn}	general element of A in microstrain/(kgf or kgf.m)
a_{mno}	single load response portion of a_{mn} in microstrain/(kgf or kgf.m)
k_{mnF_i}	combined load interaction contribution to a_{mn} in microstrain/(kgf^2 or kgf^2.m or kgf^2.m^2) where F_i can be V, D, S, M_V, M_D or M_S.
$k_{mn\delta}$	influence of oleo deflection on a_{mn} in microstrain/(kgf.m or kgf.m^2)
δ	oleo deflection in m
+, -	as superscripts indicate positive or negative load parameter respectively
T	as superscript indicates the transpose of the vector
$\{\bar{\varepsilon}\}$	intermediate strain vector during iterative procedure
(o),o	as superscript and subscript respectively indicate the initial value before iteration
1	as subscript indicates values after the first iteration
$E_m(i)$	intermediate parameter values used to determine final calibration parameters in microstrain/(kgf or kgf^2 or kgf.m)
$S_m(i)$	title given to the set of strains from a particular calibration test case, i, in microstrain.

1. INTRODUCTION

As part of a programme intended to assess the effects of heavyweight take-offs on the RAAF's Mirage IIIO aircraft, strain gauges have been attached to a test main undercarriage which is to be installed in a test aircraft for use in a series of flight trials. The purpose of these gauges is to determine the wheel loads experienced by the undercarriage during take off in the heavyweight condition. Knowing the loads, the stresses at potentially critical areas can then be determined by calculation.

This procedure of using strain gauges to determine the applied wheel loads, rather than to measure directly the stresses in the potentially critical areas themselves, was adopted primarily because of the large number of such areas; for example, in ref. 1 are listed 34 potentially critical areas on each leg, and it was not practicable to attach gauges to all of these. An additional reason for adopting the present procedure is that a knowledge of the wheel loads is useful in interpreting the factors which are actually inducing the stresses.

This memorandum is concerned, firstly, with a laboratory calibration of the undercarriage in which prescribed loads were applied and the resultant strains measured. From this calibration it is possible to establish the elements a_{mn} of a matrix A such that

$$\{\varepsilon\} = A\,\{F\} \qquad (1)$$

where $\{\varepsilon\}$ is the vector comprising the measured strains,

and $\{F\}$ is the vector comprising the applied loads.

In the flight trials the strains are to be measured and the loads are to be determined from them. A procedure for achieving this is also described. As will be seen, because of non-linearities in the system, this involves more than a simple inversion of eqn. (1).

2. STRAIN GAUGE POSITIONS AND LOADING SYSTEM

2.1 Positioning of Strain Gauge Transducers

The applied wheel loads on an undercarriage can in general be specified by six quantities (three orthogonal forces and moments) acting at a defined loading point. Due to expected tyre deflections during the flight trials making the lines of application of forces uncertain, the general set of applied loads (including three moments)

---

1. L. Szarski, Mirage III Fatigue Investigation: Analysis of Main Undercarriage - Definitions of Stress Relations for Potentially Critical Sections, CAC Report No. AA170.

was used in the calibration tests, requiring six independent strain gauge transducers for the calibration of each leg. The gauge positions for the starboard leg are shown in Fig. 1. (The gauges for the port leg are in corresponding locations). Specifically,

(i) Gauge 1 measures tensile or compressive strain and is mounted on the outboard face of the lower leg 203 mm above the axle centre-line, and is oriented parallel to the longitudinal axis of the lower leg.

(ii) Gauge 2 measures tensile or compressive strain and is mounted on the inboard face of the lower leg 263 mm above the axle centre-line, and is oriented parallel to the longitudinal axis of the lower leg.

(iii) Gauge 3 measures shear strain and is mounted on the outboard face of the lower leg 224 mm above the axle centre-line, and is oriented transverse to the longitudinal axis of the lower leg.

(iv) Gauge 4 measures axial strain and is mounted on the side strut casing 335 mm from the end of the casing.

(v) Gauge 5 measures axial strain and is mounted on the drag brace 139 mm from the point of attachment to the pintle beam.

(vi) Gauge 6 measures bending strain and is mounted on the fore and aft faces of the lower leg 254 mm above the axle centre-line and is oriented parallel to the longitudinal axis of the lower leg.

Ref. 2 shows the gauge positions in more detail and a cross-reference between the gauge numbering system used in this memorandum and that in ref. 2 is given in Table 1.

2. ARL DRG-No. 10839, Mirage Heavyweight Take-off Trials - Layout Main Undercarriage Transducers Locations 31-36 Port & Stbd. A3-76, 20 May 1977.

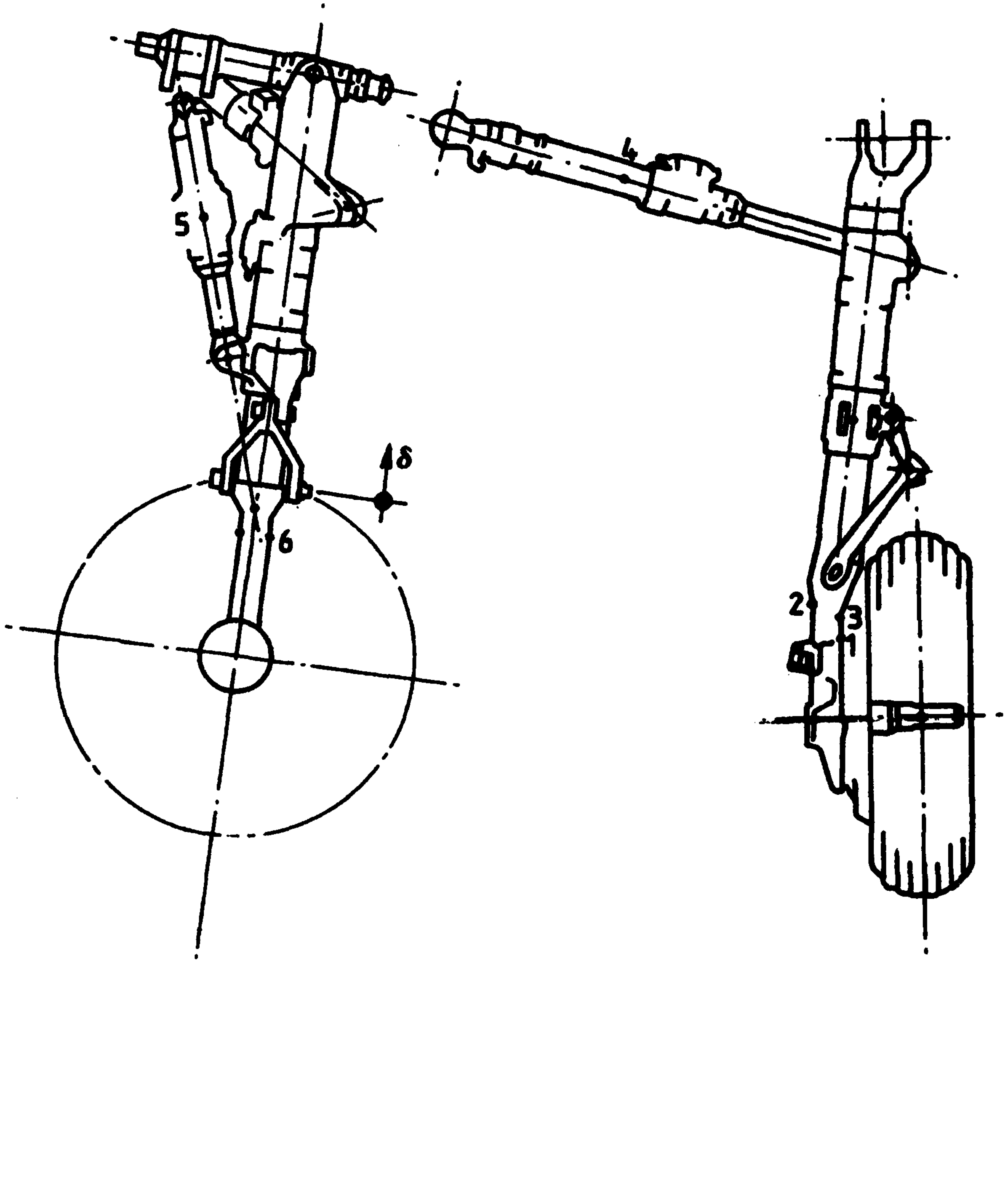

FIG. 1 : STRAIN GAUGE LOCATIONS—STARBOARD LEG

TABLE 1

GAUGE NO. IN THIS MEMORANDUM	GAUGE NO. IN REF. 2
1	31
2	32D
3	33
4	34
5	35
6	37
ROTARY POTENTIOMETER	36

In addition to the strain gauges a rotary potentiometer was attached at the junction of the torque link and the oleo casing to measure the deflections of the oleo leg.

2.2 Definition of Applied Loads

The six components of the ground-to-wheel load which acts on the undercarriage are illustrated in Fig. 2 and are defined as follows:

V:- Vertical load applied at the intersection point of the axle and axle retaining bolt centre-lines, acting normal to the axle and parallel to the oleo centre-line in side view; positive upwards.

D:- Drag load applied at the point of application of V, acting normal to the axle and to V; positive aft.

S:- Side load applied at the point of application of V and D, acting normal to V and D; positive outboard.

M_V, M_D, M_S Moments about V, D and S axes respectively; for the port leg, positive directions are given by the right hand screw rule but for the starboard leg positive directions are given by the left hand screw rule.

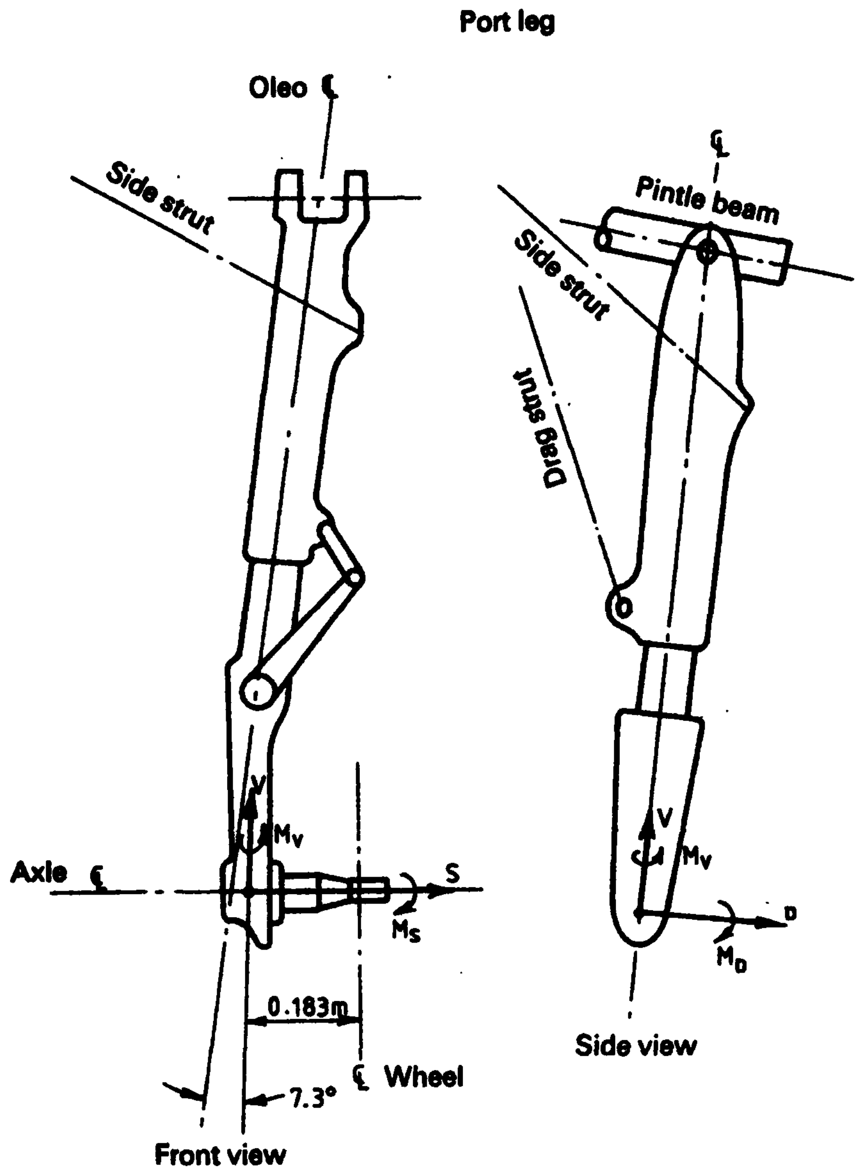

FIG. 2: WHEEL LOAD COMPONENTS ON PORT LEG

The sign convention of the wheel load components is illustrated in Fig. 3. The above definitions need to be qualified by consideration of the effects of the deflections which the undercarriage undergoes when loaded. These deflections cause the relationship between the wheel load axes and the aircraft axes to vary with applied wheel load. To overcome this, the point of application of the loads is considered to be fixed to the axle rather than fixed relative to the aircraft C of G, while the directions of the load axes remain parallel to those of the undeflected leg. Therefore, as the leg deflects, the point of load application moves relative to the aircraft C of G but the directions of the load axes do not alter. Further, although the directions of the wheel load components are defined relative to the axle and oleo centre-lines to conform with definitions used in previous calibration tests on this undercarriage (ref. 3), it is more practical, for testing purposes, to interpret the definitions in terms of the mounting points of the undercarriage to the aircraft. These mounting points are subject to far less variation from their design geometry than the leg, in practice, and thus the load axes can be related more accurately to the aircraft axes. The relative orientations of the load and aircraft axes are shown in Fig. 4.

In previous calibration tests (ref. 3) the load application point was defined as the wheel centre. However, preliminary tests in this series showed a non-linear response of the strain gauges to side load when it was applied strictly according to the definition of ref. 3. By re-defining the load application point as the intersection of the axle and axle retaining bolt centre-lines, the non-linearity in the side load response was eliminated and this definition of the loading point is used for the presentation of all results in this memorandum.

3. CALIBRATION PROCEDURE

3.1 Principle of the Method

The output of the gauges on a leg can be related to the applied loads on the leg by the matrix eqn. (1); written out at length this is

$$\begin{bmatrix} \varepsilon_1 \\ \varepsilon_2 \\ \varepsilon_3 \\ \varepsilon_4 \\ \varepsilon_5 \\ \varepsilon_6 \end{bmatrix} = \begin{bmatrix} a_{11} & a_{12} & a_{13} & a_{14} & a_{15} & a_{16} \\ a_{21} & a_{22} & a_{23} & a_{24} & a_{25} & a_{26} \\ a_{31} & a_{32} & a_{33} & a_{34} & a_{35} & a_{36} \\ a_{41} & a_{42} & a_{43} & a_{44} & a_{45} & a_{46} \\ a_{51} & a_{52} & a_{53} & a_{54} & a_{55} & a_{56} \\ a_{61} & a_{62} & a_{63} & a_{64} & a_{65} & a_{66} \end{bmatrix} \begin{bmatrix} V \\ D \\ S \\ M_V \\ M_D \\ M_S \end{bmatrix} \qquad (2)$$

3. H. Gorjanicyn, Mirage Fatigue Investigation, Method of Evaluating Landing Gear Loads From Flight Test Recordings, CAC Report AA159, 10 November 1967.

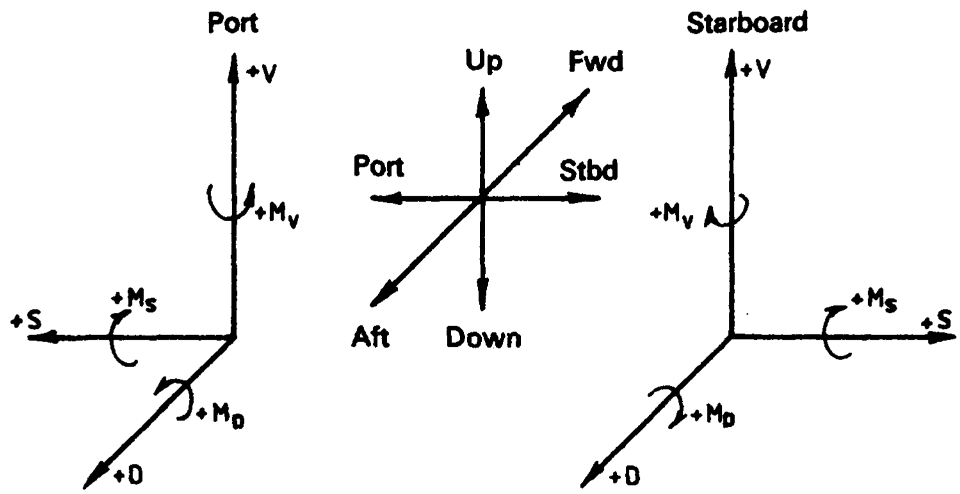

FIG. 3: LOADING SIGN CONVENTION

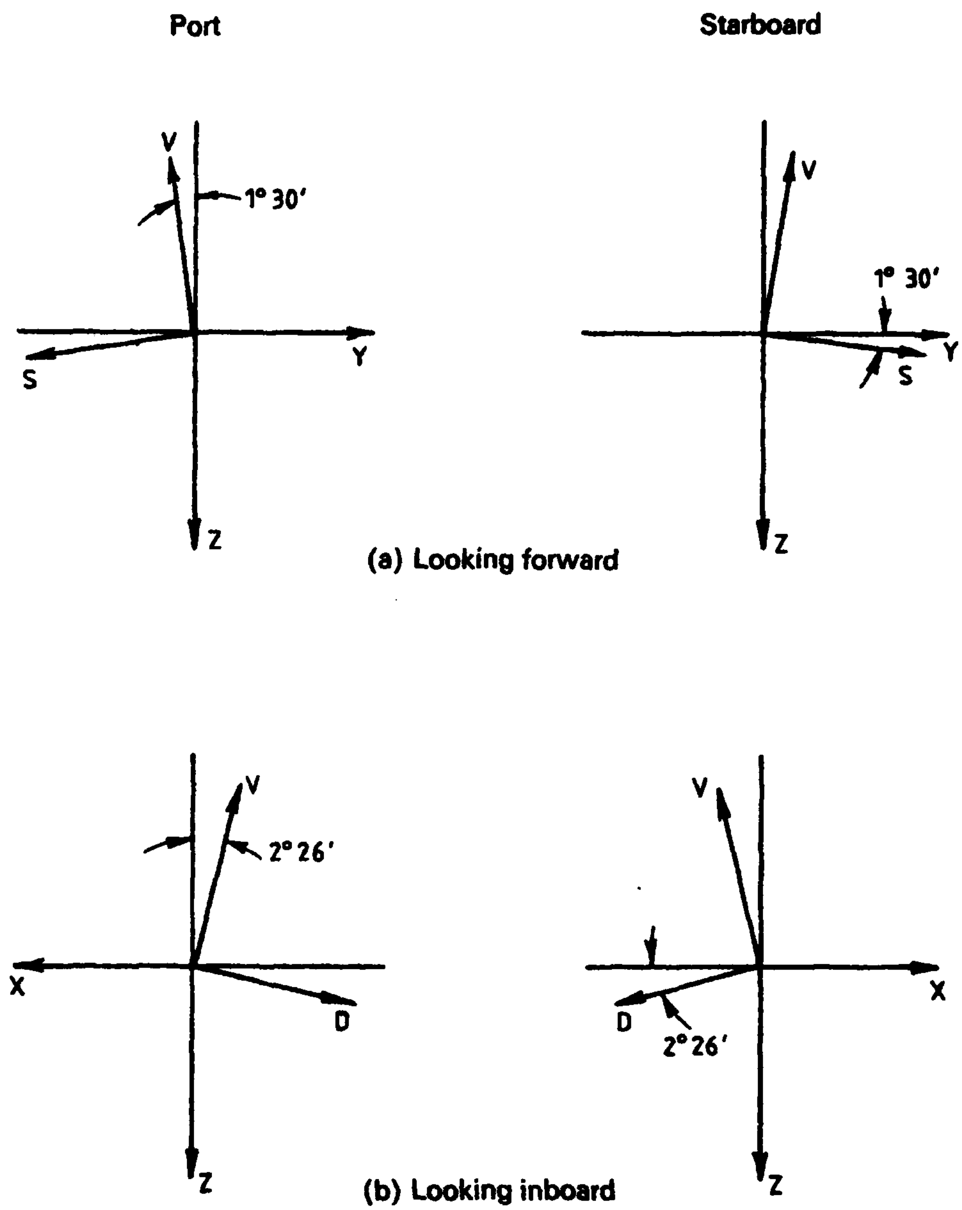

FIG. 4: RELATION BETWEEN LOAD AXES AND AIRCRAFT AXES

In a truly linear system each of the a_{mn} would be a constant and would simply be the measured response of the mth gauge to unit value of the nth load, with all other loads zero. However in the present case non-linearities can arise because of the significant deflections which occur. Account can be taken of these non-linearities by assuming that the a_{mn} are no longer constants but are linear functions of the applied loads and the oleo deflection δ. Typically, then, one would write

$$a_{mn} = a_{mno} + k_{mnV} V + k_{mnD} D + k_{mnS} S$$

$$+ k_{mnMV} M_V + k_{mnMD} M_D + k_{mnMS} M_S + k_{mn\delta} \delta \qquad (3)$$

However, this introduces 36 X 8 = 288 constants and the determination of all these would be exceptionally time consuming. Further, on physical grounds, many of these can be expected to be small and may therefore be eliminated. The terms that were eliminated and the reasons for so doing are detailed below.

The terms k_{m1V}, k_{m2D}, k_{m3S}, k_{m4MV}, k_{m5MD}, k_{m6MS} (m = 1 to 6) are eliminated because their presence implies a quadratic response to application of a single load. However, the main non-linearities are associated with the interactive effects under combined loads and there was no evidence in the tests of non-linear behaviour under a single load.

Gauges 1, 2, 3 and 6 are all located on the lower leg and the deflection of the loading point relative to this part of the structure is unaffected by oleo deflection. Hence the terms $k_{mn\delta}$ (m = 1, 2, 3, 6; n = 1 to 6) are eliminated.

Since, in practice, the three moments are expected to be relatively small, the terms k_{mnMV}, k_{mnMD}, k_{mnMS} (m = 1 to 6, n = 1 to 6) are eliminated as are the terms k_{mnV}, k_{mnD}, k_{mnS} (m = 1 to 6, n = 4, 5, 6) and the terms $k_{4n\delta}$, $k_{5n\delta}$ (n = 4, 5, 6) i.e. all the second order terms associated with moments are eliminated.

Also it is assumed that there is no interaction between the drag and side loads so that k_{m2S} and k_{m3D} (m = 1 to 6) are eliminated.

Finally, when two loads are applied in combination it cannot be discerned which load is affecting the other, only that the two loads interact. For example consider the strain, ε_2, produced when side and vertical loads are applied in combination:

$$\varepsilon_2 = (a_{210} + k_{21S} S) V + (a_{230} + k_{23V} V) S \qquad (4)$$

i.e. $\varepsilon_2 = a_{210}\, V + a_{230}\, S + (k_{21S} + k_{23V})\, VS$ (5)

It may be assumed that only one of k_{21S} and k_{23V} is non-zero without affecting the result. Here it will be the practice to take any such k whose final suffix is D or S as zero i.e., k_{21S} in the above example. (Because of the previous eliminations, this covers all the relevant cases).

Thus, after making the above eliminations equations (2) become:

$$\varepsilon_1 = a_{110}\, V + (a_{120} + k_{12V}\, V)\, D + (a_{130} + k_{13V}\, V)\, S + a_{140}\, M_V + a_{150}\, M_D + a_{160}\, M_S$$

$$\varepsilon_2 = a_{210}\, V + (a_{220} + k_{22V}\, V)\, D + (a_{230} + k_{23V}\, V)\, S + a_{240}\, M_V + a_{250}\, M_D + a_{260}\, M_S$$

$$\varepsilon_3 = a_{310}\, V + (a_{320} + k_{32V}\, V)\, D + (a_{330} + k_{33V}\, V)\, S + a_{340}\, M_V + a_{350}\, M_D + a_{360}\, M_S$$

$$\varepsilon_4 = (a_{410} + k_{41\delta}\, \delta)\, V + (a_{420} + k_{42V}\, V + k_{42\delta}\, \delta)\, D + (a_{430} + k_{43V}\, V + k_{43\delta}\delta\,)\, S + a_{440}\, M_V + a_{450}\, M_D + a_{460}\, M_S$$

$$\varepsilon_5 = (a_{510} + k_{51\delta}\, \delta)\, V + (a_{520} + k_{52V}\, V + k_{52\delta}\, \delta)\, D + (a_{530} + k_{53V}\, V + k_{53\delta}\, \delta)\, S + a_{540}\, M_V + a_{550}\, M_D + a_{560}\, M_S$$

$$\varepsilon_6 = a_{610}\, V + (a_{620} + k_{62V}\, V)\, D + (a_{630} + k_{63V}\, V)\, S + a_{640}\, M_V + a_{650}\, M_D + a_{660}\, M_S$$

(6)

The various a's and k's appearing in equations (6) are the quantities determined from the calibration tests.

3.2 Test procedure

The test undercarriage was mounted on a special rig (Fig. 5) which consisted of a heavy baseplate with attached anchors for the ends of the pintle beam and side strut. The design of the rig was such that the undercarriage configuration was the same as for an aircraft installation and the baseplate of the rig lay in the S-D plane of the applied loads of this memorandum. For the tests, the baseplate of the rig was clamped to a horizontal surface with the undercarriage upside down as illustrated in Fig. 6 (in which the load cell set up at the end of the axle should be disregarded as it was not used in these tests). This enabled the applied loads to be interpreted for testing purposes in the following manner:

V:- Vertical load acting vertically through the intersection point of the axle and axle retaining bolt centre-lines; positive downwards.

D:- Drag load acting horizontally through the application point of V and parallel to the printle beam in plan view; positive away from the drag brace.

S:- Side force acting horizontally through the application point of V and D and normal to the pintle beam; positive away from the side strut.

With the baseplate of the rig clamped to a rigid horizontal floor bed the loads were applied to the undercarriage by hydraulic jacks which were anchored at one end and attached to the undercarriage at the other by a shackle. The jacks were operated in tension and the load applied by a jack was measured by incorporating a load cell link somewhere between the jack anchor point and the shackle. It was necessary to use different shackle shapes for the various applied load components. The shackles and their method of attachment to the undercarriage leg are sketched in Figure 7. The shackles for the side and drag loads enabled them to be applied through the defined loading point, but it was not possible to do this with the vertical load due to congestion of the undercarriage and mounting rig vertically below the loading point. The reference point for application of the vertical load was the wheel centre (0.183 m outboard along the axle centre line from the defined loading point). Although application of vertical load through this reference point represents a combined loading case of V and M_D, it is referred to in this memorandum as just a vertical load case but treated as a combined loading case for data reduction. The separation of the vertical load shackle from the drag and side load shackles allowed drag or side load to be applied in combination with vertical load without difficulty. It would have required a special shackle to apply drag and side load in combination, but this was not pursued as it was not expected to be an important load case.

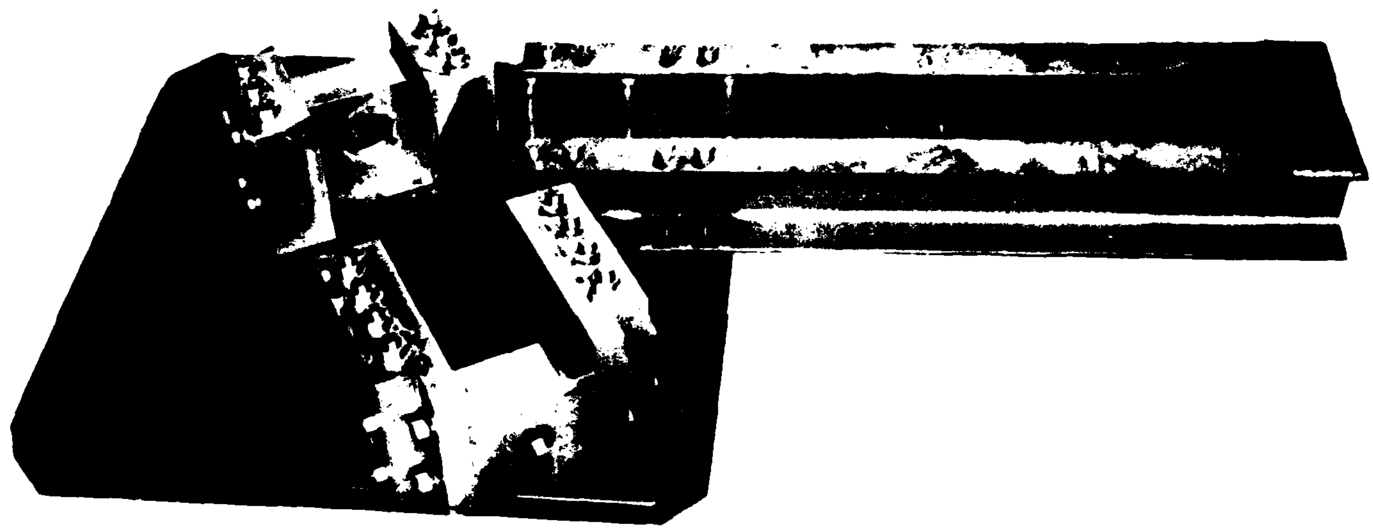

FIG. 5: UNDERCARRIAGE MOUNTING RIG

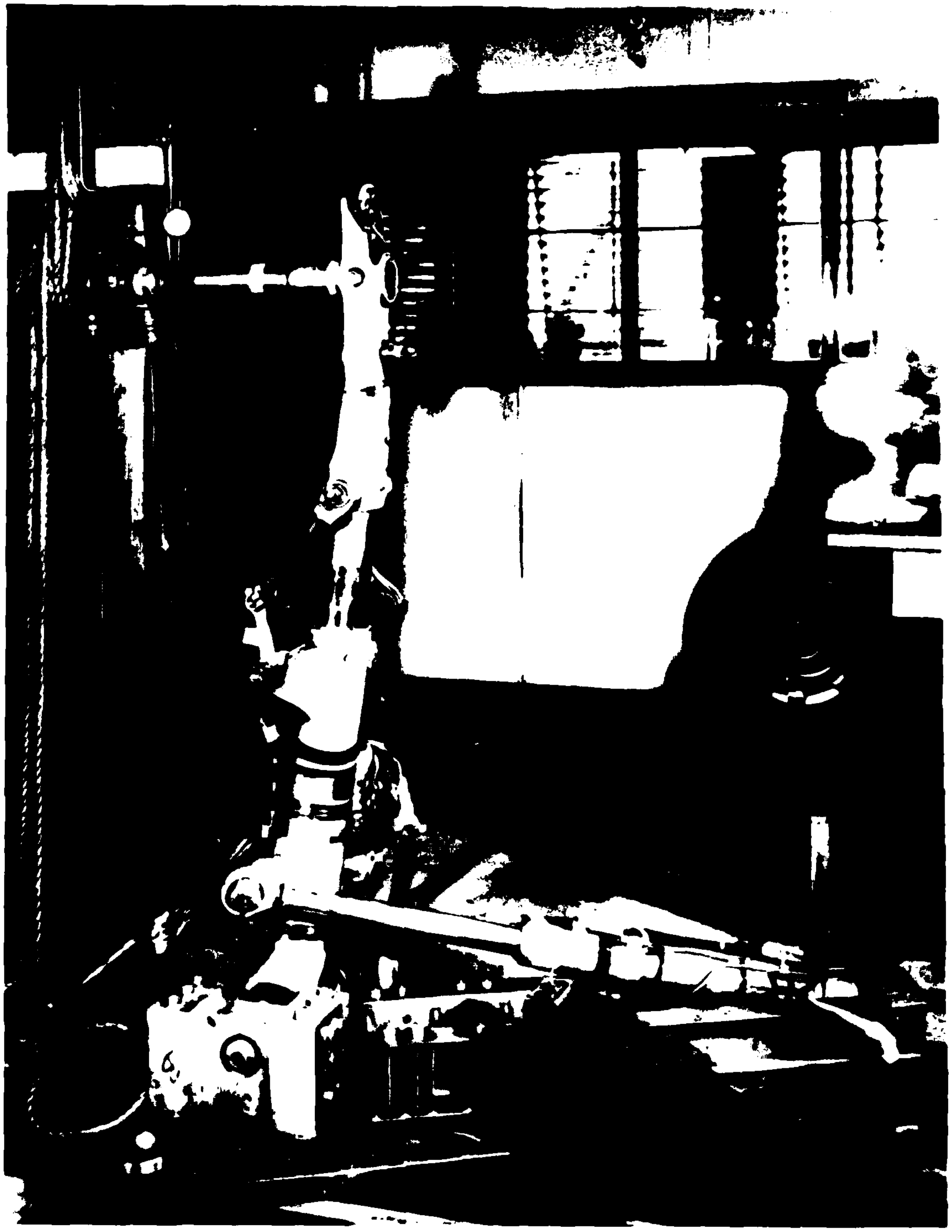

FIG. 6: TEST SETUP

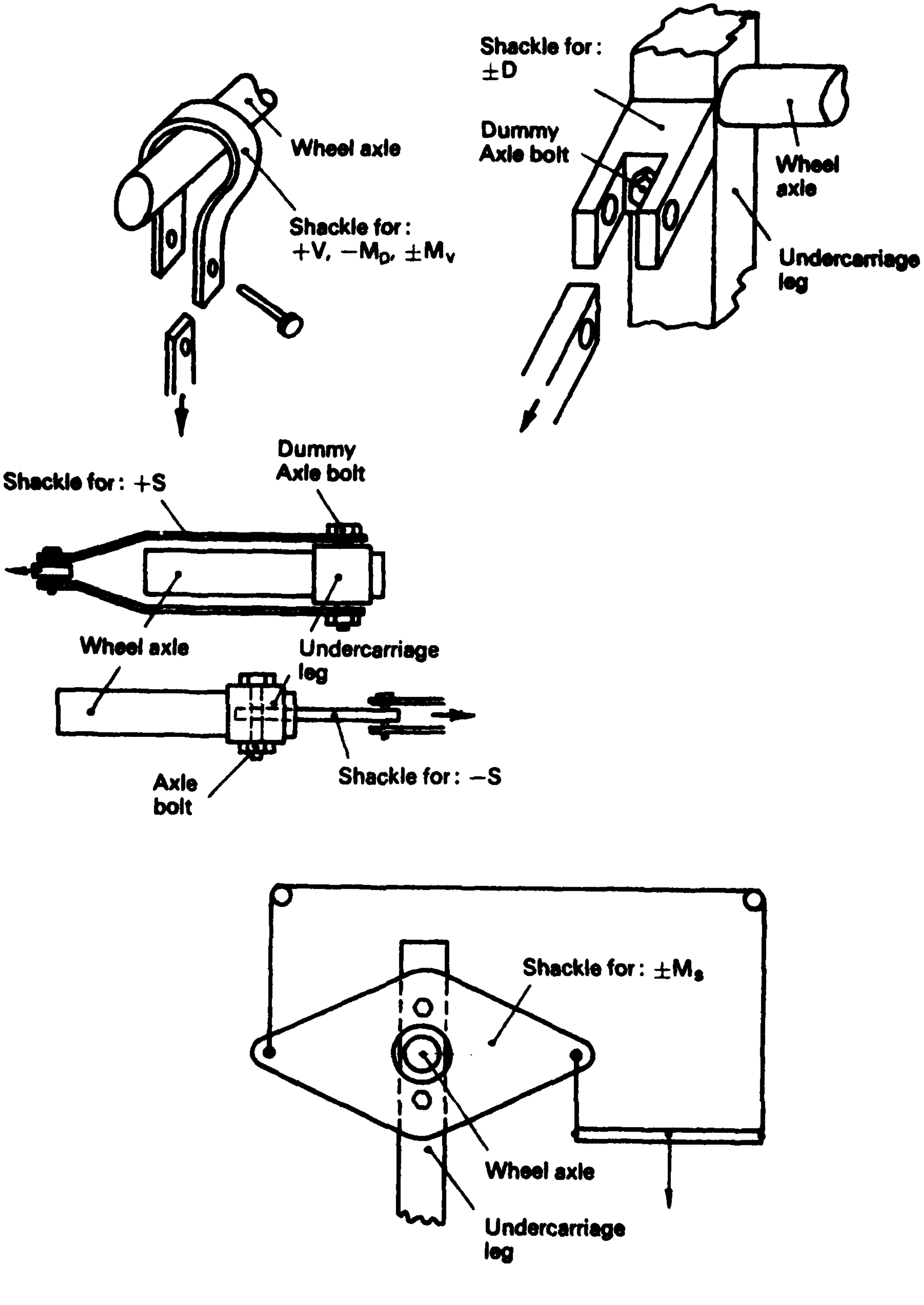

FIG. 7: SHACKLES

The aim of the test procedure was for the loads in each test to be applied according to their definitions at at least one reading point, and that at this point the applied loads and the strains in the undercarriage be accurately measured and recorded. To achieve the first part of this aim, the approach was adopted of checking the drag and side load jacks with an inclinometer to ensure they were horizontal at the reading point, and of checking the vertical load with a plumbob to ensure it was vertical at the reading point. Further, the horizontal state of the floor bed was checked with an inclinometer and care was taken in positioning the jack anchor points to ensure that the side load jack was perpendicular to the pintle beam and the drag load jack was parallel to it. In combined loading cases and/or in cases where significant oleo deflections occurred, it was necessary to offset the jack anchor points at the start of loading so that, at the reading point, the loads were in accordance with their definitions. The necessary offsets were determined by measuring the deflections in a prior dummy run.

To achieve the second part of the aim of the test procedure, the load level was held as constant as possible while the strains were recorded at the reading point. Also, the strain gauges were calibrated before each test run and zero strain levels read at the beginning and end of each run. The calibration of the load cell amplifiers was periodically checked.

It has been the experience in previous tests on this undercarriage (Ref. 3), and confirmed in these tests, that consistently different calibration parameters result from the application of positive and negative values of the same load component. One possible explanation of this phenomenon is that settlement of the joints in the undercarriage effectively creates different structures for positive and negative loading. Regardless of the explanation, positive and negative tests were done for D, S and M_V and both sets of results are presented in this memorandum. It was inconvenient, and not considered worthwhile, to test for both positive and negative values of the other load components or combined load effects.

The test sequence used and the parameters from eqns. (6) consequently obtained are given below:-

(i) Positive V applied at the wheel centre (0.183 m outboard of the defined loading point), with zero, then non-zero, oleo deflections. From these two sets of results the $k_{m1\delta}$ (m = 4, 5) are obtained.

(ii) Positive V applied 0.0762 m outboard of the wheel centre, with zero oleo deflection. From these results taken with those obtained in (i), the a_{m10} and a_{m50} (m = 1 to 6) are obtained.

(iii) Positive and negative D applied through the defined loading point from which the a_{m20} ($m = 1$ to 6) are obtained.

(iv) Positive and negative D applied through the wheel centre. From these results taken with those obtained in (iii), the a_{m40} ($m = 1$ to 6) are obtained.

(v) Positive and negative S applied through the defined loading point from which the a_{m30} ($m = 1$ to 6) are obtained.

(vi) Positive M_S from which the a_{m60} ($m = 1$ to 6) are obtained.

(vii) Positive V through the wheel centre combined with positive and negative S through the defined loading point, with zero and non-zero oleo deflection. From these results the $k_{m3\delta}$ ($m = 4, 5$) and k_{m3V} ($m = 1$ to 6) are obtained.

(viii) Positive V combined with positive and negative D through the respective points of application in (vii), with zero and non-zero oleo deflection. From these results the $k_{m2\delta}$ ($m = 4, 5$) and k_{m2V} ($m = 1$ to 6) are obtained.

The above test sequence was applied to both the port and starboard undercarriage legs. Loads were applied in four or five increments before the maximum load was reached. In combined load tests one load was applied first up to its maximum and then held constant while the other load was applied up to its maximum. In some of the tests the final reading point at maximum load was the only valid calibration reading, due to initial jack anchor offset as explained previously. Multiple tests were done in some cases to check the consistency of the calibration parameters. Oleo deflection was controlled by the order of load application in combined load tests e.g. in a combined V and S test, if S was applied first it tended to lock-up the oleo and delay its collapse under V.

3.3 Test Results

The results of the calibration and the calculation of the various parameters from these are given at length in Appendix I. A summary of these results is given in Tables 2 and 3 below. Table 2 is for positive loads only, or for both positive and negative loads where no separate negative load parameter was obtained. Table 3 is for negative loads only. The units used throughout are as follows:

V, D, S in kgf

M_V, M_D, M_S in kgf.m

δ in m

$\epsilon_1, \ldots, \epsilon_6$ in microstrain

a_{mn} ($n = 1,2,3$) in microstrain/kgf

a_{mn} ($n = 4,5,6$) in microstrain/kgf.m

TABLE 2. CALIBRATION RESULTS FOR POSITIVE LOAD

PARAMETER	STARBOARD LEG	PORT LEG
a_{11}	-0.0186	-0.0441
a_{21}	-0.0339	-0.0037
a_{31}	0.0072	-0.0068
a_{41}	$-0.0724 + 0.0805\delta$	$-0.0451 + 0.0533\delta$
a_{51}	$0.0200 - 0.0258\delta$	$0.0091 - 0.0062\delta$
a_{61}	0.0089	-0.0036
a_{12}	$0.0121 + 0.04 \times 10^{-5}V$	$-0.0081 - 0.07 \times 10^{-5}V$
a_{22}	$-0.0040 + 0.06 \times 10^{-5}V$	$0.0044 + 0.06 \times 10^{-5}V$
a_{32}	$-0.2731 - 1.76 \times 10^{-5}V$	$0.2785 + 0.36 \times 10^{-5}V$
a_{42}	$0.0220 + 0.02 \times 10^{-5}V - 0.008\delta$	$0.0096 - 0.90 \times 10^{-5}V + 0.259\delta$
a_{52}	$0.3818 + 0.56 \times 10^{-5}V - 0.413\delta$	$0.3821 + 0.68 \times 10^{-5}V - 0.640\delta$
a_{62}	$0.3059 + 0.30 \times 10^{-5}V$	$0.3079 + 0.17 \times 10^{-5}V$
a_{13}	$-0.2665 - 0.99 \times 10^{-5}V$	$-0.2631 - 1.00 \times 10^{-5}V$
a_{23}	$0.4746 + 1.93 \times 10^{-5}V$	$0.4681 + 1.84 \times 10^{-5}V$
a_{33}	$-0.0019 + 0.22 \times 10^{-5}V$	$-0.0158 - 0.05 \times 10^{-5}V$
a_{43}	$0.4668 + 1.35 \times 10^{-5}V - 0.44\delta$	$0.4666 + 1.44 \times 10^{-5}V - 0.44\delta$
a_{53}	$-0.1418 - 0.55 \times 10^{-5}V + 0.19\delta$	$-0.1301 - 0.49 \times 10^{-5}V + 0.17\delta$
a_{63}	$0.0021 + 0.02 \times 10^{-5}V$	$0.0206 + 0.05 \times 10^{-5}V$
a_{14}	0.025	0.002
a_{24}	0.070	-0.089
a_{34}	-4.092	4.189
a_{44}	-0.013	-0.082
a_{54}	-0.016	-0.021
a_{64}	0.079	-0.057
a_{15}	1.33	1.27
a_{25}	-1.85	-1.81
a_{35}	-0.088	0.034
a_{45}	-0.424	-0.358
a_{55}	0.147	0.096
a_{65}	0.076	-0.072
a_{16}	0.050	0.000
a_{26}	-0.010	-0.013
a_{36}	-0.236	0.217
a_{46}	0.021	0.017
a_{56}	0.286	0.286
a_{66}	1.172	1.194

TABLE 3: CALIBRATION RESULTS FOR NEGATIVE LOAD

PARAMETER	STARBOARD LEG	PORT LEG
a_{12}	$0.0069 + 0.04 \times 10^{-5}V$	$-0.0105 - 0.07 \times 10^{-5}V$
a_{22}	$0.0041 + 0.06 \times 10^{-5}V$	$-0.0055 + 0.06 \times 10^{-5}V$
a_{32}	$-0.2796 - 1.76 \times 10^{-5}V$	$0.2435 + 0.36 \times 10^{-5}V$
a_{42}	$0.0244 + 0.02 \times 10^{-5}V - 0.008\delta$	$-0.0039 - 0.90 \times 10^{-5}V + 0.259\delta$
a_{52}	$0.3763 + 0.56 \times 10^{-5}V - 0.413\delta$	$0.3630 + 0.68 \times 10^{-5}V - 0.640\delta$
a_{62}	$0.3018 + 0.30 \times 10^{-5}V$	$0.2978 + 0.17 \times 10^{-5}V$
a_{13}	$-0.2654 - 0.99 \times 10^{-5}V$	$-0.2636 - 1.00 \times 10^{-5}V$
a_{23}	$0.4674 + 1.93 \times 10^{-5}V$	$0.4674 + 1.84 \times 10^{-5}V$
a_{33}	$-0.0019 + 0.22 \times 10^{-5}V$	$-0.0158 - 0.05 \times 10^{-5}V$
a_{43}	$0.4531 + 1.35 \times 10^{-5}V - 0.44\delta$	$0.4541 + 1.44 \times 10^{-5}V - 0.44\delta$
a_{53}	$-0.1418 - 0.55 \times 10^{-5}V + 0.19\delta$	$-0.1323 - 0.49 \times 10^{-5}V + 0.17\delta$
a_{63}	$0.0021 + 0.02 \times 10^{-5}V$	$0.0206 + 0.05 \times 10^{-5}V$
a_{14}	0.036	-0.036
a_{24}	0.032	-0.013
a_{34}	-3.945	4.291
a_{44}	-0.019	0.032
a_{54}	-0.014	0.024
a_{64}	0.081	-0.005

3.4 Deflections

In addition to the oleo deflection, during some of the tests deflections of the defined loading point were measured using a vernier tape. Deflections were not monitored rigorously for all load cases and so limited results only are presented in Table 4 below.

TABLE 4 - MEASURED DEFLECTIONS OF LOAD POINT

APPLIED LOAD COMPONENT	DIRECTION OF MEASURED DEFLECTION	MAGNITUDE PER UNIT LOAD
V	SIDE	-0.3×10^{-5} m/kgf
D	DRAG	1.5×10^{-5} m/kgf
S	SIDE	3.8×10^{-5} m/kgf
M_D	SIDE	-3.6×10^{-5} m/kgf.m

The values in Table 4 apply to both the port and starboard legs and for positive and negative loading. It should be noted that lateral deflections due to V and M_D, as listed in Table 4, apply for zero oleo deflection. Lateral deflection due to oleo deflection has been calculated from the geometry of the undercarriage leg to be 0.13δ (the oleo makes an angle of 82.7° with the axle). Similarly the vertical deflection is 0.99δ. The deflection of the defined loading point is important for determining the stresses in the undercarriage from the wheel loads calculated from the measured strains.

4. DETERMINATION OF LOADS FROM FLIGHT TEST DATA

4.1 General Procedure

The calibration tests serve to determine the coefficients in eqns. (6); then, in the flight tests the strains and oleo deflection are measured and it is required to solve eqns. (6) for the loads. These can be written as

$$\{\varepsilon\} = A\,\{F\} \tag{7}$$

where $\{\varepsilon\}^T = (\varepsilon_1, \ldots, \varepsilon_6)$, (7)

$\{F\}^T = (F_1, \ldots, F_6)$

and A is the calibration matrix.

Because the equations are non-linear a solution cannot be achieved by a direct inversion. Instead, an iterative procedure is used as described below.

(i) Initially all the cross-product terms are ignored in (6) so that the equations are linearised to the form

$$\{\varepsilon\} = A_o\{F\} \tag{8}$$

where a typical element of A_o has the form

$$a_{mn}^{(o)} = a_{mno} + k_{mn\delta}\ \delta \tag{9}$$

with a_{mno} and $k_{mn\delta}$ being the values applicable to positive loads.

(ii) On solving eqns. (8), a first approximation $\{F_o\}$, say, is obtained for the applied load vector.

(iii) Using the value of $\{F_o\}$, the A_o matrix is updated to A_1 to allow for cross-product terms and the sense of the load components.

(iv) Now form the strain vector $\{\varepsilon\}$, as given by

$$\{\bar{\varepsilon}\} = A_1\ \{F\} \tag{10}$$

(v) Form the difference

$$\{\Delta\varepsilon\} = \{\varepsilon\} - \{\bar{\varepsilon}\} \tag{11}$$

If this is sufficiently small, then $\{F_o\}$ may be regarded as a satisfactory approximation to $\{F\}$ and the process stopped. The present criterion for a satisfactory approximation is that each element in $\{\Delta\varepsilon\}$ should be less, in absolute value, than 0.5 microstrain, this being chosen to conform with the accuracy of the strain gauge data.

(vi) If the difference in (11) is not sufficiently small the iteration process is continued by solving

$$\{\Delta\varepsilon\} = A_1\ \{\Delta F\} \tag{12}$$

for $\{\Delta F\}$. This gives a new value

$$\{F_1\} = \{F_o\} + \{\Delta F\} \tag{13}$$

for the load vector and one can return to stage (iii) and repeat the process.

It has been found that this method usually converges in no more than three iterations. A flow chart for the associated computer program, MIR3UC, is shown in Fig. 8. Program MIR3UC has been entered in the ARL Computer Program Register and full details of the program are contained therein.

4.2 Accuracy of Procedure

An appraisal of the accuracy of the above procedure is best done in two parts: firstly by applying it to arbitrarily chosen data for which the exact solution is known, and then by applying it to the strain gauge data actually obtained in the calibration tests. From the first application, the general validity of the iterative method of solution can be assessed whilst, from the second, an indication is given of the size of errors likely to be encountered in practice.

(i) Prescribed Data

If an arbitrary set of loads (which need not have any connection either with those loads used in the calibration tests or those likely to be encountered in service) is assumed then the corresponding exact values of strains can be calculated directly by evaluating the righthand sides of eqns. (6). These strains may then be used as input data for the program MIR3UC and the point of interest is whether the loads output by the program agree with those originally assumed. The results of two such calculations are shown in Table 5 below.

TABLE 5: SAMPLE CHECKS ON ACCURACY OF ITERATIVE METHOD

LOAD COMPONENT	STARBOARD LEG			PORT LEG		
	ASSUMED LOAD VECTOR	CALCULATED LOAD VECTOR	% ERROR IN LOAD	ASSUMED LOAD VECTOR	CALCULATED LOAD VECTOR	% ERROR IN LOAD
V	3628.8	3631.4	0.07	2721.6	2722.3	0.03
D	1134.0	1134.1	0.01	-1360.8	-1361.0	0.01
S	1360.8	1361.3	0.04	-1285.8	-1285.8	0.00
M_V	207.4	207.4	0.00	0.0	0.0	-
M_D	-663.6	-663.5	0.02	-497.7	-497.5	0.04
M_S	230.4	230.4	0.00	0.0	0.1	-
δ	0.0762			0.0		
STRAIN COMPONENT	STRAIN VECTOR			STRAIN VECTOR		
ε_1	-1329.6			-361.3		
ε_2	1855.9			230.7		
ε_3	-1192.4			-358.1		
ε_4	724.4			-540.2		
ε_5	250.4			-354.9		
ε_6	631.4			-413.7		

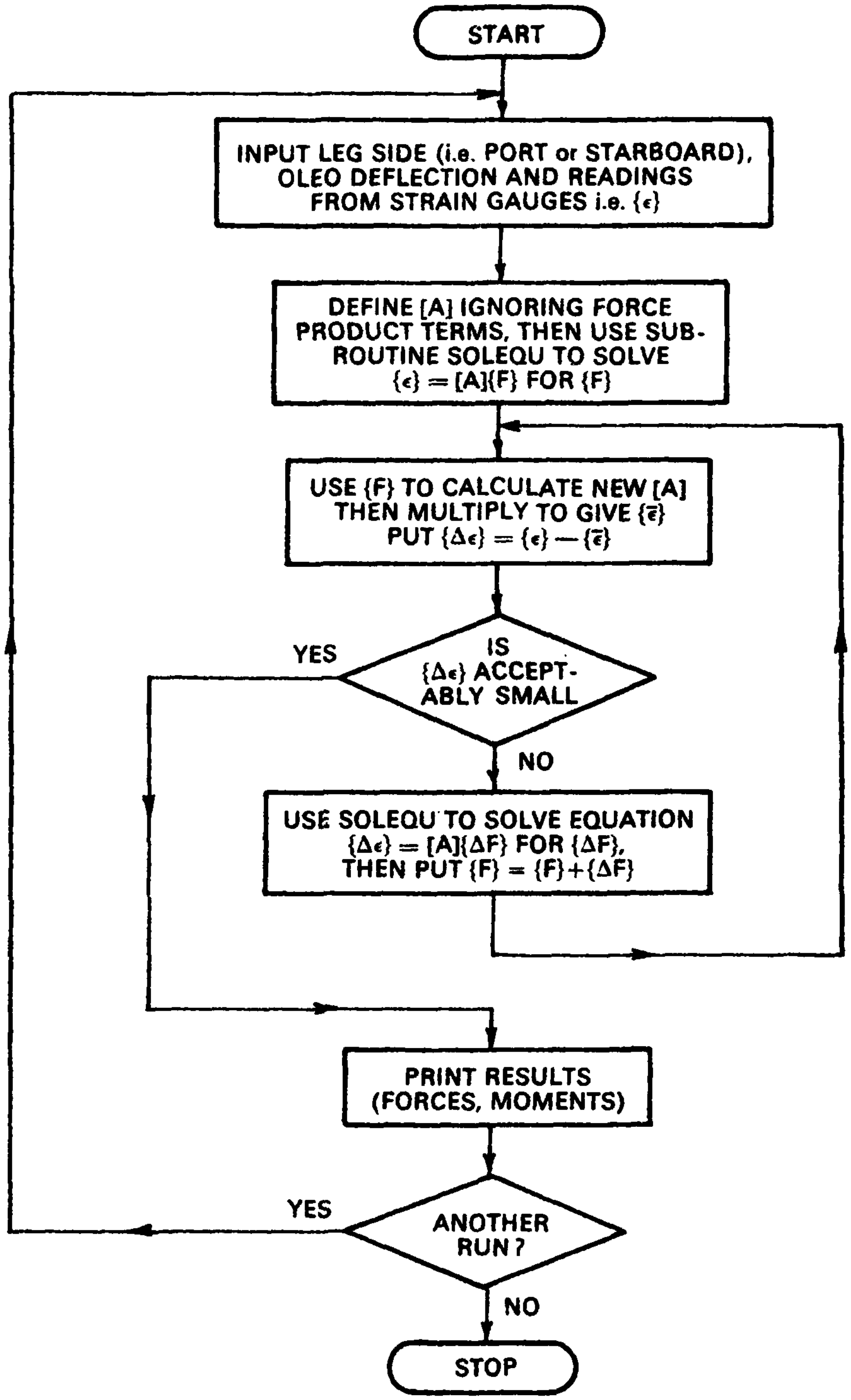

FIG. 8: FLOWCHART FOR PROGRAM "MIR3UC"

Comparison of the exact and calculated values shows excellent agreement, the maximum difference being 0.07%. This serves to validate the computer program and gives confidence in the accuracy of the iterative procedure on which it is based.

(ii) Calibration Data

As a further test of the general procedure, the strains as measured in some of the calibration runs were used as input data to the program MIR3UC and the output loads were compared with those actually applied in the calibration. The results of this comparison are shown in Table 6 for the starboard leg and Table 7 for the port leg. The agreement is reasonable except in the case of the starboard leg under combined V, M_D and S loads. There, the calculated vertical load is quite badly in error and there are significant errors in the calculated side load also. The reasons for these errors are taken up in Section 5.

TABLE 6: COMPARISON OF EXPERIMENTAL AND CALCULATED LOADS FOR STARBOARD LEG

APPLIED LOADS	δ (m)	V (kgf)		D (kgf)		S (kgf)	
		TEST	CALC.	TEST	CALC.	TEST	CALC.
V, $-M_D$	0	2268.0	2305.0	0.0	12.8	0.0	0.9
V, $-M_D$	.0754	3628.8	3528.8	0.0	13.4	0.0	-35.1
V, $-M_D$	0	2721.6	2753.1	0.0	0.3	0.0	6.7
-D	0	0.0	9.9	-1360.8	-1362.3	0.0	1.9
+D, $+M_V$	0	0.0	0.1	1134.0	1133.6	0.0	-0.1
+S	0	0.0	-49.9	0.0	8.8	1360.8	1354.0
V, $-M_D$, +S	0	2721.6	1929.5	0.0	-21.7	1360.8	1248.0
V, $-M_D$, -S	.0762	3628.8	3197.5	0.0	9.6	-1360.8	-1459.2
V, $-M_D$, + D	0	2721.6	[illegible]36.6	1360.8	1347.2	0.0	3.7
V, $-M_D$, + D	.0785	3628.8	3453.8	1360.8	1361.1	0.0	-12.3

TABLE 7: COMPARISON OF EXPERIMENTAL AND CALCULATED LOADS FOR PORT LEG

APPLIED LOADS	δ (m)	V (kgf)		D (kgf)		S (kgf)	
		TEST	CALC.	TEST	CALC.	TEST	CALC.
V, $-M_D$	0	1814.4	1908.7	0.0	0.5	0.0	22.9
V, $-M_D$	.0894	3628.8	3601.8	0.0	-11.6	0.0	28.2
V, $-M_D$	0	2721.6	2742.4	0.0	-0.3	0.0	2.9
-D	0	0.0	-1.1	-2041.2	-2041.0	0.0	0.0
+D, $+M_V$	0	0.0	0.7	2041.2	2041.1	0.0	0.0
+S	0	0.0	-2.7	0.0	5.1	1360.8	1361.3
V, $-M_D$, + S	0	2721.6	2718.4	0.0	-17.6	1236.5	1255.2
V, $-M_D$, -S	.1013	3628.8	3554.4	0.0	6.3	-1313.2	-1292.9
V, $-M_D$, +D	0	2721.6	2778.7	1318.0	1315.3	0.0	6.9
V, $-M_D$, +D	.0848	3628.8	3574.3	1307.1	1312.4	0.0	-5.2

4.3 Sensitivity Analysis

With strain gauge data there may be a significant degree of variation between readings taken in nominally identical situations, especially if the data are at the low end of the effective range of the gauges. With small variations in absolute value causing significant percentage changes in data values, it is undesirable for large changes in results derived from the data to occur due to these variations.

A check for this was made using the arbitrary load cases set out in Table 5. A set of six strain vectors was formed by reducing each strain component in turn by 10% and leaving the five other strain components unchanged. These six strains vectors were then used as input to MIR3UC and

and the resulting {F} vectors were compared with their original values in Table 5. These results are presented in Tables 8 and 9.

TABLE 8: SENSITIVITY CHECK - STARBOARD LEG

MICROSTRAIN			CALCULATED LOAD WITH STRAIN COMPONENT REDUCED					
STRAIN COMPONENT REDUCED	VALUE FROM TABLE 5	VALUE AFTER 10% REDUCTION	V	D	S	M_V	M_D	M_S
NONE	-	-	3631.4	1134.1	1361.3	207.4	-663.5	230.4
ε_1	-1329.6	-1196.6	-1283.0	1137.4	633.7	219.5	-821.8	292.8
ε_2	1855.9	1670.3	9487.3	1169.1	2124.4	191.3	-314.0	133.4
ε_3	-1192.4	-1073.2	3542.4	1130.0	1347.5	178.7	-668.3	234.7
ε_4	724.4	652.0	2977.2	1058.4	1073.2	214.6	-743.9	263.2
ε_5	250.4	225.4	3659.4	1051.1	1369.2	212.9	-661.1	252.0
ε_6	631.4	568.3	3545.9	1196.7	1351.3	207.2	-665.8	163.4
δ	0.0762							

TABLE 9: SENSITIVITY CHECK - PORT LEG

MICROSTRAIN			CALCULATED LOAD WITH STRAIN COMPONENT REDUCED					
STRAIN COMPONENT REDUCED	VALUE FROM TABLE 5	VALUE AFTER 10% REDUCTION	V	D	S	M_V	M_D	M_S
NONE	-	-	2722.3	-1361.0	-1285.8	0.0	-497.5	0.1
ε_1	-361.3	-325.2	1862.8	-1383.6	-1390.1	-1.3	-513.0	2.0
ε_2	230.7	207.6	3128.0	-1350.2	-1226.3	0.5	-474.1	-0.1
ε_3	-358.1	-322.3	2710.9	-1360.2	-1285.6	8.5	-498.0	0.2
ε_4	-540.2	-486.2	2956.2	-1300.0	-1115.7	-2.0	-452.1	-14.6
ε_5	-354.9	-319.4	2709.8	-1242.1	-1277.0	-5.5	-494.8	-30.2
ε_6	-413.7	-372.3	2716.1	-1394.6	-1291.0	-0.2	-499.4	43.2
δ	0.0							

Both tables show drastic changes in some components of load (especially V) due to the 10% changes in one strain component. Changes in ε_1 and ε_2 cause very large changes in V and significant changes also in S, M_D and M_S. A change in ε_4 also causes significant changes in V, S and M_D. This high sensitivity poses several problems as it requires a high degree of accuracy in the strain gauge data which may be unrealistic to expect. The implifications of this will be discussed in the next section.

5. DISCUSSION

The results of the calibration tests are not as reliable as is desirable and pose problems in regard to their use in analysing flight test data. It has been demonstrated that the loads, most specially the vertical load, as calculated from strains using the calibration parameters, are highly sensitive to variations in the input strains (Tables 8 and 9). This sensitivity was further confirmed by the poor accuracy with which some of the test loads were calculated from the test strains (Tables 6 and 7). Normally, with calibration parameters calculated from the test loads and strains, one would expect that the test loads would be calculated very accurately from the test strains, as with the prescribed data (Table 5). However, where the calibration parameters were obtained by averaging the results of multiple tests of the same load case, the loads of a particular test as obtained from the strain values of that test sometimes differed by in excess of 20% from the actual applied loads. In view of the fact that in-flight tests will be done under less precisely controlled conditions than the laboratory calibration tests, errors can be expected in the in-flight strain gauge data due to zero drifts, etc. Hence, the wheel loads calculated from these data would be expected to be highly inaccurate, with errors probably greater than 20% in the vertical load.

It has been mentioned that the equations formed by the calibration parameters are ill-conditioned. This is due to the fact that none of the strain gauges on the leg respond strongly to vertical load. The vertical load is then effectively determined by separating a small uniform axial strain from large bending strains out of strains ε_1 and ε_2 on the lower part of the leg. In an ideal set-up each strain gauge would respond strongly to one load component and weakly to all other load components. This aim is partially fulfilled by the gauges in that

ε_3 responds to M_V,

ε_4 responds to S,

ε_5 responds to D,

ε_6 responds to M_S,

but ε_1 and ε_2 respond to M_D and S.

In order to improve the system it is required that gauges ε_1 and ε_2 be replaced by two gauges, one of which responds to M_D and the other to V. A gauge which responded to M_D could be either ε_1 or ε_2 or a new gauge which measured bending strain. Whether the gauge measured bending strain or tensile strain it is desirable that it be positioned as close to the axle as practicable so as to reduce the bending influence of the side load. A gauge responding to the vertical load is a more difficult proposition. It is desirable for the gauge to be in a position where the vertical load produces a reasonable strain but the other load components produce lesser strains. Positions on the lower part of the leg could be used by having a strain gauge bridge which separated the axial strain from the bending strain, but the axial strain would be small and so data errors would cause significant errors in V. From the lower part of the leg the axial strain is transferred through the oleo in a complex and unpredictable manner and no site along the oleo causing is suitable. The vertical load is then transferred into the pintle beam as a bending load. It is possible to find a suitable site on the pintle beam where there is a large bending strain due to vertical load and lessor strains due to other load components. However the pintle beam is at the remote end of the oleo strut from the wheel axle and dynamic effects, with possible phase shifts between different components, would mean that a measure of vertical load at the pintle beam was not a good indicator of what was happening at the wheel. Hence it is probably more realistic to measure the vertical load at a site on the lower part of the leg and accept the errors caused by a lack of response of the gauge. To this end the current system of gauges could be retained with 20% error in the vertical load and 5% error in the other load components accepted. Alternatively an effort could be made to improve the system by shifting gauge ε_1 down to as close to the wheel axle as possible and replacing gauge ε_2 by a strain gauge bridge located on the neutral axis for M_D, as close to the wheel axle as possible, with two gauges on opposite surfaces of the leg and the output of the bridge being the sum of two gauges. In this position the latter pair of strain gauges would be vulnerable to physical damage during aircraft operations, and means should be devised for protecting them.

The assumption that the interference between load components is linear is considered to be reasonable in view of the fact that the interference effects are small in comparison to the single load parameters. The assumption of linear interference is valid provided the assumptions of small deflection theory in structural analysis are not violated, i.e. at load levels greater than in the calibration tests which will be experienced during heavyweight take-offs the interference effects may become non-linear.

6. FUTURE DEVELOPMENTS

In view of the sensitivity of the current system to data errors it is considered necessary to replace gauges ε_1 and ε_2 with two new gauges. It is pointless to do any further tests with the current system of gauges. If further tests are done all single load parameters should be tested again and also combined load interactions should be tested more fully, with combined side and drag load and possibly all three force components combined. The tests should be done to higher load levels, approaching those expected in flight trials. Also during further tests, deflections of the loading point should be monitored in all tests where possible. Every endeavour should be made to ensure the load components are applied in accordance with their definitions using the rig monitoring techniques described in this memorandum. Also maximum accuracy from the instrumentation should be achieved by run-by-run monitoring of the zero drifts and calibration constants of both the strain gauge and load cell amplifiers.

7. CONCLUSIONS

A procedure has been developed whereby the wheel loads sustained by the Mirage undercarriage in flight trials can be determined from the output of six strain gauges. However, the present arrangement of gauges is such that errors of up to 20% could be made in the determination of the vertical loads. The situation could be improved by relocating two of the gauges but this would necessarily involve recalibration of the undercarriage.

CALIBRATION RESULTS

In the following, all strain gauge outputs are cited as microstrain, distances in metres, forces in kgf and moments in kgf.m.

A. STARBOARD LEG

(i) Vertical load at wheel centre

TABLE A1

LOADS	$V=2268.0$ kgf; $M_D=-0.183V$ kgf.m. $D=S=M_V=M_S=\delta=0$					
RUN	ε_1	ε_2	ε_3	ε_4	ε_5	ε_6
1	-588.5	681.8	61.0	8.9	-17.5	-10.7
2	-593.7	688.3	39.7	9.2	-11.4	-13.0
3	-594.3	689.6	55.7	17.6	-18.2	-13.1
MEAN MICROSTRAIN	-592.2	686.6	52.1	11.9	-15.7	-12.3
MICROSTRAIN/ UNIT V	-0.2611	0.3027	0.0230	0.0052	-0.0069	-0.0054

The last row in Table A1 gives the quantities

$$E_m(1) = a_{m10} - 0.183\, a_{m50},\ m = 1 \text{ to } 6 \qquad \text{(A1)}$$

the E_m denoting microstrain per unit load.

TABLE A2

LOADS	V=3628.8 kgf, M_D=-0.183V kgf.m; δ=0.0754m; D=S=M_V=M_S=0					
RUN	ε_1	ε_2	ε_3	ε_4	ε_5	ε_6
1	-944.5	1100.7	99.8	41.5	-36.0	-12.5
2	-953.7	1112.0	68.4	36.3	-25.8	-16.6
3	-963.2	1125.6	89.5	45.4	-34.7	-20.7
MEAN MICROSTRAIN	-953.8	1112.8	85.9	41.1	-32.2	-16.6
MICROSTRAIN/ UNIT V	-0.2628	0.3067	0.0237	0.0113	-0.0089	-0.0046

The last row in Table A2 gives the quantities

$$E_m\ (2) = a_{m10} - 0.183\ a_{m50},\quad m = 1,\ 2,\ 3,\ 6 \qquad \text{(A2)}$$

$$E_m\ (2) = (a_{m10} + 0.0754\ k_{m1\delta}) - 0.183\ a_{m50}.\quad m = 4,5 \qquad \text{(A3)}$$

by subtracting the m = 4 case of eqn. (A1) from that of eqn. (A3), $k_{41\delta}$ is determined:

$$k_{41\delta} = (0.0113 - 0.0052)/0.0754 = 0.0805$$

Similarly,

$$k_{51\delta} = (-0.0089 + 0.0069)/0.0754 = -0.0258$$

For m = 1, 2, 3, 6, an average value of the E_m in Tables A1 and A2 can be calculated for later use. Thus

$$E_m\ (3) = (E_m\ (1) + E_m\ (2))/2,\quad m = 1,\ 2,\ 3,\ 6 \qquad \text{(A4)}$$

$$E_m\ (3) = E_m\ (1)\quad ,\ m = 4,\ 5 \qquad \text{(A5)}$$

$$\text{where } E_m\ (3) = a_{m10} - 0.183\ a_{m50} \qquad \text{(A6)}$$

The values of E_m (3) calculated from eqns. (A4) and (A5) are listed in Table A3.

TABLE A3

$E_m(3)$	$E_1(3)$	$E_2(3)$	$E_3(3)$	$E_4(3)$	$E_5(3)$	$E_6(3)$
MICROSTRAIN/ UNIT V	-0.2620	0.3047	0.0233	0.0052	-0.0069	-0.0050

(ii) Vertical load 0.0762m outboard of wheel centre

TABLE A4

LOADS	V=2721.6 kgf; M_D=-0.2592V kgf.m; D=S=M_V=M_S=δ=0					
RUN	ϵ_1	ϵ_2	ϵ_3	ϵ_4	ϵ_5	ϵ_6
1	-989.6	1212.6	81.7	102.3	-49.4	-29.3
MICROSTRAIN/ UNIT V	-0.3636	0.4455	0.0300	0.0376	-0.0182	-0.0108

The last row in Table A4 gives the quantities

$$E_m(4) = a_{m10} - 0.2592\, a_{m50}, \quad m = 1 \text{ to } 6 \qquad (A7)$$

By subtracting eqn. (A6) from eqn. (A7), the a_{m50} are determined. For example,

$$a_{150} = (-0.3636 + 0.2620)/0.0762 = 1.33$$

Similarly,

$$a_{250} = -1.85$$

$$a_{350} = -0.088$$

$$a_{450} = -0.424$$

$$a_{550} = 0.147$$

$$a_{650} = 0.076$$

With the a_{m50} determined, the a_{m10} can be determined from eqn. (A6); thus,

$$a_{110} = -0.2620 + 0.183 \times 1.33 = -0.0186$$

Similarly,

$$a_{210} = -0.0339$$

$$a_{310} = 0.0072$$

$$a_{410} = -0.0724$$

$$a_{510} = 0.0200$$

$$a_{610} = 0.0089$$

(iii) Drag load at defined loading point

TABLE A5

LOADS	D=1360.8 kgf; $V=S=M_V=M_D=M_S=\delta=0$					
RUN	ε_1	ε_2	ε_3	ε_4	ε_5	ε_6
1	16.5	-5.4	-371.7	29.9	519.5	416.2
MICROSTRAIN/ UNIT D	0.0121	-0.0040	-0.2731	0.0220	0.3818	0.3059

TABLE A6

LOADS	$D=-1360.8$ kgf; $V=S=M_V=M_D=M_S=\delta=0$					
RUN	ε_1	ε_2	ε_3	ε_4	ε_5	ε_6
1	-10.7	-4.2	380.6	-32.9	-513.0	-411.3
2	-8.2	-6.9	380.4	-33.5	-511.2	-410.2
MEAN MICROSTRAIN	-9.5	-5.6	380.5	-33.2	-512.1	-410.8
MICROSTRAIN/ UNIT D	0.0069	0.0041	-0.2796	0.0244	0.3763	0.3018

The last row in Table A5 gives the quantities a_{m20}, m = 1 to 6, for positive loading and the last row in Table A6 gives the quantities a_{m20}, m = 1 to 6, for negative loading.

(iv) Drag load at the wheel centre

TABLE A7

LOADS	$D=1134.0$ kgf; $M_V=0.183D$ kgf.m; $V=S=M_D=M_S=\delta=0$					
RUN	ε_1	ε_2	ε_3	ε_4	ε_5	ε_6
1	18.9	10.0	-1158.9	22.2	429.6	363.3
MICROSTRAIN/ UNIT D	0.0167	0.0088	-1.0220	0.0196	0.3788	0.3204

TABLE A8

LOADS	$D=-1360.8$ kgf; $M_V=0.183D$ kgf.m; $V=S=M_D=M_S=\delta=0$					
RUN	ε_1	ε_2	ε_3	ε_4	ε_5	ε_6
1	-18.3	-13.6	1363.0	-28.5	-508.6	-430.9
MICROSTRAIN/ UNIT D	0.0134	0.0100	-1.0016	0.0209	0.3738	0.3167

The last row of Tables A7 and A8. for positive and negative loading respectively, gives the quantities

$$E_m\ (5) = a_{m20} + 0.183\ a_{m40},\quad m = 1 \text{ to } 6 \qquad \text{(A8)}$$

By subtracting the last row of Tables A5 and A6 from the last row of Tables A7 and A8 respectively, and dividing by the moment arm from the wheel centre to the defined loading point, the a_{m40} are determined. For example

$$a_{140}^{+} = (0.0167 - 0.0121)/0.183 = 0.025$$

$$a_{140}^{-} = (0.0134 - 0.0069)/0.183 = 0.036$$

Similarly,

$a_{240}^{+} = 0.070$ $\qquad$ $a_{240}^{-} = 0.032$

$a_{340}^{+} = -4.092$ $\qquad$ $a_{340}^{-} = -3.945$

$a_{440}^{+} = -0.013$ $\qquad$ $a_{440}^{-} = -0.019$

$a_{540}^{+} = -0.016$ $\qquad$ $a_{540}^{-} = -0.014$

$a_{640}^{+} = 0.079$ $\qquad$ $a_{640}^{-} = 0.081$

(v) Side load at defined loading point.

TABLE A9

LOADS	S=1360.8 kgf; $V=D=M_V=M_D=M_S=\delta=0$					
RUN	ε_1	ε_2	ε_3	ε_4	ε_5	ε_6
1	-363.1	645.9	60.4	633.6	-195.7	-9.3
2	-361.9	645.5	33.2	635.5	-191.7	-5.4
3	-362.9	645.9	33.4	636.6	-191.7	-5.5
MEAN MICROSTRAIN	-362.6	645.8	42.3	635.2	-193.0	-6.7
MICROSTRAIN/ UNIT S	-0.2665	0.4746	0.0311*	0.4668	-0.1418	-0.0049**
PARAMETER NAME	a_{130}^+	a_{230}^+	a_{330}^+	a_{430}^+	a_{530}^+	a_{630}^+

TABLE A10

LOADS	S=-1360.8 kgf; $V=D=M_V=M_D=M_S=\delta=0$					
RUN	ε_1	ε_2	ε_3	ε_4	ε_5	ε_6
1	361.8	-636.6	1.9	-616.3	192.7	-2.7
2	360.4	-635.3	3.3	-616.8	193.1	-3.0
MEAN MICROSTRAIN	361.1	-636.0	2.6	-616.6	192.9	-2.9
MICROSTRAIN/ UNIT S	-0.2654	0.4674	-0.0019	0.4531	-0.1418	0.0021
PARAMETER NAME	a_{130}^-	a_{230}^-	a_{330}^-	a_{430}^-	a_{530}^-	a_{630}^-

Positive side load was applied by a crude shackle which had the potential to introduce torques to the leg. It is considered that this is the reason for the discrepancy between positive and negative values of a_{330} and a_{630}. For this reason it was decided to take

$$a_{330}^{+} = a_{330}^{-} = -0.0019 \ ^{*}$$

and $$a_{630}^{+} = a_{630}^{-} = 0.0021 \ ^{**}$$

(vi) Positive M_S

TABLE A11

LOADS	M_S=230.4 kgf.m; V=V=S=M_V=M_D=δ=0					
RUN	ε_1	ε_2	ε_3	ε_4	ε_5	ε_6
1	11.5	-2.3	-54.3	4.9	65.8	270.0
MICROSTRAIN/ UNIT M_S	0.050	-0.010	-0.236	0.021	0.286	1.172
PARAMETER NAME	a_{160}	a_{260}	a_{360}	a_{460}	a_{560}	a_{660}

(vii) Combined vertical and side loads

TABLE A12

LOADS	V=2721.6 kgf; M_D=-0.183V kgf.m; S=1360.8 kgf; D=M_V=M_S=δ=0					
RUN	ε_1	ε_2	ε_3	ε_4	ε_5	ε_6
1	-1108.3	1568.5	111.5	703.3	-236.3	-17.5
ELIMINATE V AND M_D	-395.2	739.2	48.1	689.1	-217.5	-3.9
ELIMINATE S (A9-3)	-32.3	93.3	14.7	52.5	-25.8	1.6
MICROSTRAIN/ VxS	-0.87×10^{-5}	2.52×10^{-5}	0.40×10^{-5}	1.42×10^{-5}	-0.70×10^{-5}	0.04×10^{-5}

The measured strains listed in Table A12 represent the quantities

$$S_m\ (1) = a_{m10}V + a_{m50}M_D + \overset{+}{a}_{m30}S + \overset{+}{k}_{m3V}VS, \ m = 1 \text{ to } 6 \qquad \text{(A9)}$$

In order to solve eqn. (A9) for $\overset{+}{k}_{m3V}$, the first three terms have to be eliminated from the right hand side and then the equation divided by the product VS. As the equation indicates, each term can be eliminated by subtracting the product of the value of the applied load component as listed in the table and the appropriate parameter value as determined previously. This represents the general approach to elimination but two other approaches are also occasionally used in this appendix. Firstly it is convenient to eliminate V and M_D simultaneously since, in all combined load tests, the vertical load was applied through the wheel centre. Thus

$$M_D = -0.183V$$

$$a_{m10}V + a_{m50}M_D = (a_{m10} - 0.183a_{m50})V, \ m = 1 \text{ to } 6 \qquad \text{(A10)}$$

Values of $(a_{m10} - 0.183a_{m50})$, m = 1 to 6, are contained in Table A3. Secondly, in some of the combined load tests, the type and sequence of loading was such that the second applied load did not significantly deflect the line of action of the first applied load. Therefore, in such cases, the intermediate stage before the second load is applied, represents a valid single load calibration of the first applied load and so was included as a run in a previous table of single load tests. In these cases it is then more accurate to eliminate the intermediate single load strains from the final strain rather than to use the calculated parameter which represents an average of all single load test runs. By eliminating the intermediate strains, any inaccuracies in the application of the first load permeating through to the final combined load strains will be eliminated. For example, to eliminate S in Table A12 the strains from run 3 in Table A9 were subtracted as this run was the intermediate stage of the combined load test. If this method of elimination had not been used, the errors mentioned in section (v) would not have been eliminated from the combined load strains. Throughout the remainder of this appendix, if a load is eliminated by subtracting intermediate strains of a test, those strains will be referenced to a previous table and run number, listed in brackets in the current table, e.g. in Table A12, ELIMINATE S (A9-3) indicates that the side load is eliminated by subtracting the strains of run 3 in Table A9. The last row of Table A12 gives the quantities

$$E_m\ (6) = \overset{+}{k}_{m3V}, \ m = 1 \text{ to } 6 \qquad \text{(A11)}$$

TABLE A13

LOADS	$V=3628.8$ kgf; $M_D=-0.183V$ kgf.m; $S=1360.8$ kgf; $\delta=0.0762$m; $D=M_V=M_S=0$					
RUN	ε_1	ε_2	ε_3	ε_4	ε_5	ε_6
1	-1356.6	1832.0	141.0	701.6	-229.1	-25.3
ELIMINATE V AND M_D	-405.9	726.3	56.4	682.7	-204.0	-7.2
ELIMINATE $V\times\delta$	-405.9	726.3	56.4	660.5	-196.8	-7.2
ELIMINATE S	-43.2	80.5	14.1	25.2	-3.9	-0.5
ELIMINATE $V\times S$				-44.9	30.7	
MICROSTRAIN UNIT $V\times S$	-0.87×10^{-5}	1.63×10^{-5}	0.29×10^{-5}			-0.01×10^{-5}
MICROSTRAIN/ UNIT $S\times\delta$				-0.433	0.296	

The measured strains listed in Table A13 represent the quantities

$$S_m\ (2) = a_{m10}V+a_{m50}M_D+\overset{+}{a}_{m30}S+\overset{+}{k}_{m3V}VS,\quad m=1,2,3,6 \qquad \text{(A12)}$$

and

$$S_m\ (3) = a_{m10}V+a_{m50}M_D+k_{m1\delta}V\delta+\overset{+}{a}_{m30}S+\overset{+}{k}_{m3V}VS+\overset{+}{k}_{m3\delta}S\delta,$$
$$m=4,5 \qquad \text{(A13)}$$

Following the eliminations, the second last row of Table A13 represents the quantities

$$E_m\ (7) = \overset{+}{k}_{m3V},\quad m = 1,2,3,6 \qquad \text{(A14)}$$

and the last row of Table A13 represents the quantities

$$E_m\ (8) = k^{+}_{m3\delta},\ m = 4,5 \qquad \text{(A15)}$$

Equations (A11) and (A14) can be averaged to give

$$k^{+}_{m3V} = E_m\ (9) = (E_m(7) + E_m(6))/2,\ m = 1,2,3,6 \qquad \text{(A16)}$$

Values for k^{+}_{m3V}, m = 1 to 6, are then listed in Table A14 below

TABLE A14

k^{+}_{m3V}	k^{+}_{13V}	k^{+}_{23V}	k^{+}_{33V}	k^{+}_{43V}	k^{+}_{53V}	k^{+}_{62V}
MICROSTRAIN/ UNIT VxS	-0.87×10^{-5}	2.07×10^{-5}	0.34×10^{-5}	1.42×10^{-5}	-0.70×10^{-5}	0.02×10^{-5}

A similar procedure to Tables A12, A13 and A14 is adopted for negative side load combined with vertical load, and the results are shown below:

TABLE A15

LOADS	V=2721.6 kgf; M_D=-0.183V kgf.m; S=-1360.8 kgf; D=M_V=M_S=δ=0					
RUN	ϵ_1	ϵ_2	ϵ_3	ϵ_4	ϵ_5	ϵ_6
1	-303.5	114.8	65.9	-650.4	189.4	-18.4
ELIMINATE V AND M_D	409.6	-714.5	2.5	-664.6	208.2	-4.8
ELIMINATE S (A10-2)	49.2	-79.2	-0.8	-47.8	15.1	-1.8
MICROSTRAIN/ UNIT VxS	-1.33×10^{-5}	2.14×10^{-5}	0.02×10^{-5}	1.29×10^{-5}	-0.41×10^{-5}	0.05×10^{-5}

TABLE A16

LOADS	$V=3628.8$ kgf; $M_D=-0.183V$ kgf.m; $S=-1360.8$ kgf; $\delta=0.0762$m, $D=M_V=M_S=0$					
RUN	ε_1	ε_2	ε_3	ε_4	ε_5	ε_6
1	-546.0	399.4	78.3	-593.5	171.8	-21.8
ELIMINATE V AND M_D	404.7	-706.3	-6.3	-612.4	196.8	-3.7
ELIMINATE Vxδ	404.7	-706.3	-6.3	-634.6	204.0	-3.7
ELIMINATE S	43.6	-70.3	-8.8	-18.1	11.0	-0.8
ELIMINATE VxS				45.7	-9.2	
MICROSTRAIN/ UNIT VxS	-0.88×10^{-5}	1.42×10^{-5}	0.18×10^{-5}			0.02×10^{-5}
MICROSTRAIN/ UNIT Sxδ				-0.440	0.089	

TABLE A17

$\bar{k}_{m3V}$	$\bar{k}_{13V}$	$\bar{k}_{23V}$	$\bar{k}_{33V}$	$\bar{k}_{43V}$	$\bar{k}_{53V}$	$\bar{k}_{63V}$
MICROSTRAIN/ UNIT VxS	-1.11×10^{-5}	1.78×10^{-5}	0.10×10^{-5}	1.29×10^{-5}	-0.41×10^{-5}	0.03×10^{-5}

It is considered that the large differences between the k^{+}_{m3V} and k^{-}_{m3V} in Tables A14 and A17 and between the $k^{+}_{m3\delta}$ and $k^{-}_{m3\delta}$ in Tables A13 and A16, are due to experimental error rather than to any natural discrepancy between positive and negative load. For this reason the positive and negative values for the k_{m3V} and $k_{m3\delta}$ are averaged to give the values in Table A18 which are then applicable to positive and negative loading.

TABLE A18

k_{13V}	k_{23V}	k_{33V}	k_{43V}	k_{53V}	k_{63V}	$k_{43\delta}$	$k_{53\delta}$
-0.99×10^{-5}	1.93×10^{-5}	0.22×10^{-5}	1.35×10^{-5}	-0.55×10^{-5}	0.02×10^{-5}	-0.44	0.19

(viii) Combined vertical and drag loads.

Tests of positive and negative drag load combined with vertical load with zero and non-zero oleo deflection were performed, similarly to the combined side and vertical load tests whose results were analysed in the previous section (vii). The combined drag and vertical load test results are analysed similarly in Tables A19 to A25 below.

TABLE A19

LOADS	$V=2721.6$ kgf; $M_D=-0.183V$ kgf.m; $D=1360.8$ kgf; $S=M_V=M_S=\delta=0$					
RUN	ε_1	ε_2	ε_3	ε_4	ε_5	ε_6
1	-699.7	829.3	-383.0	42.5	518.0	414.6
ELIMINATE V AND M_D	13.4	0.0	-446.4	28.3	536.8	428.2
ELIMINATE D (A5-1)	-3.1	5.4	-74.7	-1.5	17.3	12.0
MICROSTRAIN/ UNIT VxD	-0.08×10^{-5}	0.15×10^{-5}	-2.02×10^{-5}	-0.04×10^{-5}	0.47×10^{-5}	0.32×10^{-5}

TABLE A20

LOADS	$V=3628.8$ kgf; $M_D=-0.183V$ kgf.m; $D=1360.8$ kgf; $\delta=0.0785$m; $S=M_V=M_S=0$					
RUN	ε_1	ε_2	ε_3	ε_4	ε_5	ε_6
1	-932.1	1111.2	-361.5	79.7	466.6	406.8
ELIMINATE V AND M_D	18.6	5.5	-446.1	60.8	491.6	424.9
ELIMINATE $V\times\delta$	18.6	5.5	-446.1	37.9	499.0	424.9
ELIMINATE D	2.1	10.9	-74.4	8.0	-20.6	8.7
ELIMINATE VxD				10.0	-43.8	
MICROSTRAIN/ UNIT VxD	0.04×10^{-5}	0.22×10^{-5}	-1.51×10^{-5}			0.18×10^{-5}
MICROSTRAIN/ UNIT $D\times\delta$				0.0930	-0.4098	

TABLE A21

k^{+}_{m2V}	k^{+}_{12V}	k^{+}_{22V}	k^{+}_{32V}	k^{+}_{42V}	k^{+}_{52V}	k^{+}_{62V}
MICROSTRAIN/ UNIT VxD	-0.02×10^{-5}	0.18×10^{-5}	-1.76×10^{-5}	-0.04×10^{-5}	0.47×10^{-5}	0.25×10^{-5}

TABLE A22

LOADS	V=2721.6 kgf, M_D=-0.183V kgf.m; D=-1360.8 kgf; S=M_V=M_S=δ=0					
RUN	ε_1	ε_2	ε_3	ε_4	ε_5	ε_6
1	-726.8	824.1	512.6	-22.5	-554.2	-439.3
ELIMINATE V AND M_D	-13.7	-5.2	449.2	-36.7	-535.4	-425.7
ELIMINATE D (A6-2)	-5.5	1.7	68.8	-3.2	-24.2	-15.5
MICROSTRAIN/ UNIT VxD	0.15 $\times10^{-5}$	-0.05 $\times10^{-5}$	-1.86 $\times10^{-5}$	0.09 $\times10^{-5}$	0.65 $\times10^{-5}$	0.42 $\times10^{-5}$

TABLE A23

LOADS	V=3628.8 kgf; M_D=-0.183V kgf.m; D=-1360.8 kgf; δ=0.0785m; S=M_V=M_S=0					
RUN	ε_1	ε_2	ε_3	ε_4	ε_5	ε_6
1	-962.3	1104.0	546.0	15.8	-532.1	-442.0
ELIMINATE V AND M_D	-11.6	-1.7	461.4	-3.1	-507.1	-423.9
ELIMINATE V$\times\delta$	-11.6	-1.7	461.4	-26.0	-499.7	-423.9
ELIMINATE D	-2.2	3.9	81.0	7.2	12.4	-13.2
ELIMINATE VxD				11.6	44.5	
MICROSTRAIN/ UNIT VxD	0.04 $\times10^{-5}$	-0.08 $\times10^{-5}$	-1.64 $\times10^{-5}$			0.27 $\times10^{-5}$
MICROSTRAIN/ UNIT D$\times\delta$				-0.1090	-0.4164	

TABLE A24

$k_{m2\bar{V}}$	$k_{12\bar{V}}$	$k_{22\bar{V}}$	$k_{32\bar{V}}$	$k_{42\bar{V}}$	$k_{52\bar{V}}$	$k_{62\bar{V}}$
MICROSTRAIN/ UNIT VxD	0.10×10^{-5}	-0.06×10^{-5}	-1.75×10^{-5}	0.09×10^{-5}	0.65×10^{-5}	0.34×10^{-5}

TABLE A25

k_{12V}	k_{22V}	k_{32V}	k_{42V}	k_{52V}	k_{62V}	$k_{42\delta}$	$k_{52\delta}$
0.04×10^{-5}	0.06×10^{-5}	-1.76×10^{-5}	0.02×10^{-5}	0.56×10^{-5}	0.30×10^{-5}	-0.008	-0.413

B PORT LEG

The tests conducted on the port under-carriage leg were similar to those conducted on the starboard leg and so, also, is the method of data reduction. Therefore, only the tables of values are given below for the port leg, but each table corresponds to its equivalent table number for the starboard leg and so the tables can be fully interpreted by reference to Part A of this appendix.

(i) Vertical load at wheel centre.

TABLE B1

LOADS	V=1814.4 kgf; M_D=-0.183V kgf.m; D=S=M_V=M_S=δ=0					
RUN	ϵ_1	ϵ_2	ϵ_3	ϵ_4	ϵ_5	ϵ_6
1 2	-505.0 -500.0	595.0 591.0	-24.0 -27.0	42.0 32.0	-17.0 -14.0	17.0 17.0
MEAN MICROSTRAIN	-502.5	593.0	-25.5	37.0	-15.5	17.0
MICROSTRAIN/ UNIT V	-0.2770	0.3268	-0.0141	0.0204	-0.0085	0.0094

TABLE B2

LOADS	V=3628.8 kgf; M_D=-0.183V kgf.m; δ=0.0894m; D=S=M_V=M_S=0					
RUN	ϵ_1	ϵ_2	ϵ_3	ϵ_4	ϵ_5	ϵ_6
1 2 3	-992.0 -1010.0 -1004.0	1174.0 1203.0 1195.0	-29.0 -49.0 -51.0	82.0 106.0 86.0	-26.0 -40.0 -33.0	40.0 34.0 32.0
MEAN MICROSTRAIN	-1002.0	1190.7	-43.0	91.3	-33.0	35.3
MICROSTRAIN/ UNIT V	-0.2761	0.3281	-0.0118	0.0252	-0.0091	0.0097

$$k_{41\delta} = (0.0252 - 0.0204)/0.0894 = 0.0533$$

$$k_{51\delta} = (-0.0091 + 0.0085)/0.0894 = 0.0062$$

TABLE B3

E_m (3)	E_1 (3)	E_2 (3)	E_3 (3)	E_4 (3)	E_5 (3)	E_6 (3)
MICROSTRAIN/ UNIT V	-0.2765	0.3275	-0.0130	0.0204	-0.0085	0.0096

(ii) Vertical load 0.0762m outboard of wheel centre.

TABLE B4

LOADS	$V=2721.6$ kgf $M_D=-0.2592V$ kgf.m; $D=S=M_V=M_S=\delta=0$					
RUN	ε_1	ε_2	ε_3	ε_4	ε_5	ε_6
1	-1016.1	1265.9	-42.3	129.8	-43.1	41.0
MICROSTRAIN/ UNIT V	-0.3733	0.4651	-0.0155	0.0477	-0.0158	0.0151

$$a_{150} = -(-0.3733 + 0.2765)/0.0762 = 1.27$$

$$a_{250} = -1.81$$

$$a_{350} = 0.034$$

$$a_{450} = -0.358$$

$$a_{550} = 0.096$$

$$a_{650} = 0.072$$

$$a_{110} = -0.2765 + 0.183 \times 1.27 = -0.0441$$

$$a_{210} = -0.0037$$

$$a_{310} = -0.0068$$

$$a_{410} = -0.0451$$

$$a_{510} = 0.0091$$

$$a_{610} = -0.0036$$

(iii) Drag load at defined loading point.

TABLE B5

LOADS	$D=1360.8$ kgf; $V=S=M_V=M_D=M_S=\delta=0$					
RUN	ε_1	ε_2	ε_3	ε_4	ε_5	ε_6
1	-11.0	6.0	379.0	13.0	520.0	419.0
MICROSTRAIN/ UNIT D	-0.0081	0.0044	0.2785	0.0096	0.3821	0.3079

TABLE B6

LOADS	$D=-2041.2$ kgf; $V=S=M_V=M_D=M_S=\delta=0$					
RUN	ε_1	ε_2	ε_3	ε_4	ε_5	ε_6
1	21.5	11.2	-497.0	8.0	-740.9	-607.9
MICROSTRAIN/ UNIT D	-0.0105	-0.0055	0.2435	-0.0039	0.3630	0.2978

(iv) Drag load at wheel centre.

TABLE B7

LOADS	$D=2041.2$ kgf; $M_V=0.183D$ kgf.m; $V=S=M_D=M_S=\delta=0$					
RUN	ε_1	ε_2	ε_3	ε_4	ε_5	ε_6
1	-16.0	-24.0	2133.0	-11.0	772.0	607.0
MICROSTRAIN/ UNIT D	-0.0078	-0.0118	1.0450	-0.0054	0.3782	0.2974

TABLE B8

LOADS	$D=-2041.2$ kgf; $M_V=0.183D$ kgf.m; $V=S=M_D=M_S=\delta=0$					
RUN	ε_1	ε_2	ε_3	ε_4	ε_5	ε_6
1	34.9	16.0	-2099.7	-4.0	-750.0	-606.0
MICROSTRAIN/ UNIT D	-0.0171	-0.0078	1.0287	0.0020	0.3674	0.2969

$$a^{+}_{140} = (-0.0078 + 0.0081)/0.183 = 0.002$$

$$a^{-}_{140} = (-0.0171 + 0.0105)/0.183 = -0.036$$

$a^{+}_{240} = -0.089$ $\qquad a^{-}_{240} = -0.013$

$a^{+}_{340} = 4.189$ $\qquad a^{-}_{340} = 4.291$

$a^{+}_{440} = -0.082$ $\qquad a^{-}_{440} = 0.032$

$a^{+}_{540} = -0.021$ $\qquad a^{-}_{540} = 0.024$

$a^{+}_{640} = -0.057$ $\qquad a^{-}_{640} = -0.005$

(v) Side load at defined loading point.

TABLE B9

LOADS	$S=1360.8$ kgf, $V=D=M_V=M_D=M_S=\delta=0$					
RUN	ε_1	ε_2	ε_3	ε_4	ε_5	ε_6
1	-358.0	637.0	-11.0	635.0	-177.0	22.0
MICROSTRAIN/ UNIT S	-0.2631	0.4681	-0.0081 *	0.4666	-0.1301	0.0162 **
PARAMETER NAME	a^{+}_{130}	a^{+}_{230}	a^{+}_{330}	a^{+}_{430}	a^{+}_{530}	a^{+}_{630}

TABLE B10

LOADS	$S=-1360.8$ kgf; $V=D=M_V=M_D=M_S=\delta=0$					
RUN	ε_1	ε_2	ε_3	ε_4	ε_5	ε_6
1 2	367.0 350.5	-648.0 -624.0	27.0 16.0	-622.0 -614.0	182.0 178.0	-27.0 -29.0
MEAN MICROSTRAIN	358.8	-636.0	21.5	-618.0	180.0	-28.0
MICROSTRAIN/ UNIT S	-0.2636	0.4674	-0.0158	0.4541	-0.1323	0.0206
PARAMETER NAME	a_{130}^-	a_{230}^-	a_{330}^-	a_{430}^-	a_{530}^-	a_{630}^-

take $a_{330}^+ = a_{330}^- = -0.0158$*
and $a_{630}^+ = a_{630}^- = 0.0206$**

(vi) Positive M_S

TABLE B11

LOADS	$M_S=230.4$ kgf.m; $V=D=S=M_V=M_D=\delta=0$					
RUN	ε_1	ε_2	ε_3	ε_4	ε_5	ε_6
1	0.0	-3.0	50.0	4.0	66.0	275.0
MICROSTRAIN/ UNIT M_S	0.000	-0.013	0.217	0.017	0.286	1.194
PARAMETER NAME	a_{160}	a_{260}	a_{360}	a_{460}	a_{560}	a_{660}

(vii) Combined vertical and side loads.

TABLE B12

LOADS	V=2721.6 kgf; M_D=-0.183V kgf.m; S=1236.5 kgf; D=M_V=M_S=δ=0					
RUN	ε_1	ε_2	ε_3	ε_4	ε_5	ε_6
1	-1121.0	1548.0	-53.0	692.0	-211.0	45.0
ELIMINATE V AND M_D	-368.5	656.7	-17.6	636.5	-187.9	18.9
ELIMINATE S	-43.2	77.9	-7.6	59.5	27.0	-1.2
MICROSTRAIN/ UNIT VxS	-1.28×10^{-5}	2.31×10^{-5}	-0.23×10^{-5}	1.77×10^{-5}	-0.80×10^{-5}	-0.03×10^{-5}

TABLE B13

LOADS	V=3628.8 kgf; M_D=-0.183V kgf.m; S=1165.4 kgf; δ=0.0912m; D=M_V=M_S=0					
RUN	ε_1	ε_2	ε_3	ε_4	ε_5	ε_6
1	-1356.0	1835.0	-64.0	665.0	-193.0	52.0
ELIMINATE V AND M_D	-352.6	646.6	-16.8	591.0	-162.2	17.2
ELIMINATE Vxδ	-352.6	646.6	16.8	573.3	-160.1	17.2
ELIMINATE S	-46.0	101.0	-7.4	29.6	-8.5	-1.7
ELIMINATE VxS				-45.3	25.3	
MICROSTRAIN/ UNIT VxS	-1.09×10^{-5}	2.39×10^{-5}	-0.17×10^{-5}			-0.04×10^{-5}
MICROSTRAIN/ UNIT Sxδ				-0.426	0.238	

TABLE B14

k^{+}_{m3V}	k^{+}_{13V}	k^{+}_{23V}	k^{+}_{33V}	k^{+}_{43V}	k^{+}_{53V}	k^{+}_{63V}
MICROSTRAIN/ UNIT VxS	-1.19×10^{-5}	2.35×10^{-5}	-0.20×10^{-5}	1.77×10^{-5}	-0.80×10^{-5}	-0.04×10^{-5}

TABLE B15

LOADS	V=2748.8 kgf; M_D=-0.183V kgf.m; S=-1285.8 kgf; $D=M_V=M_S=\delta=0$					
RUN	ε_1	ε_2	ε_3	ε_4	ε_5	ε_6
1	-385.5	245.0	-18.0	-567.0	153.0	-5.0
ELIMINATE V AND M_D	374.5	-655.2	17.7	-623.1	176.4	-31.4
ELIMINATE S	35.6	-54.2	-2.6	-39.2	6.3	-4.9
MICROSTRAIN/ VxS	-1.01×10^{-5}	1.53×10^{-5}	0.07×10^{-5}	1.11×10^{-5}	-0.18×10^{-5}	0.14×10^{-5}

TABLE B16

LOADS	V=3628.8 kgf; M_D=-0.183V kgf.m; S=-1313.2 kgf; δ=0.1013m; $D=M_V=M_S=0$					
RUN	ε_1	ε_2	ε_3	ε_4	ε_5	ε_6
1	-628.0	521.0	-33.0	-495.0	137.0	2.0
ELIMINATE V AND M_D	375.4	-667.4	14.2	-569.0	167.8	-32.8
ELIMINATE Vxδ	375.4	-667.4	14.2	-588.6	170.1	-32.8
ELIMINATE S	29.2	-53.6	-6.6	7.7	-3.6	-5.8
ELIMINATE VxS				60.6	-12.2	
MICROSTRAIN/ UNIT VxS	-0.61×10^{-5}	1.13×10^{-5}	0.14×10^{-5}			0.12×10^{-5}
MICROSTRAIN/ UNIT Sxδ				-0.456	0.092	

TABLE B17

$\bar{k}_{m3V}$	$\bar{k}_{13V}$	$\bar{k}_{23V}$	$\bar{k}_{33V}$	$\bar{k}_{43V}$	$\bar{k}_{53V}$	$\bar{k}_{63V}$
MICROSTRAIN/ UNIT VxS	-0.81×10^{-5}	1.33×10^{-5}	0.11×10^{-5}	1.11×10^{-5}	-0.18×10^{-5}	0.13×10^{-5}

TABLE B18

k_{13V}	k_{23V}	k_{33V}	k_{43V}	k_{53V}	k_{63V}	$k_{43\delta}$	$k_{53\delta}$
-1.00×10^{-5}	1.84×10^{-5}	-0.05×10^{-5}	1.44×10^{-5}	-0.49×10^{-5}	0.05×10^{-5}	-0.44	0.17

(viii) Combined vertical and drag loads.

TABLE B19

LOADS	$V=2721.6$ kgf; $M_D=-0.183V$ kgf.m; $D=1318.0$ kgf; $S=M_V=M_S=\delta=0$					
RUN	ε_1	ε_2	ε_3	ε_4	ε_5	ε_6
1	-770.0	902.0	359.0	36.0	505.0	442.0
ELIMINATE V AND M_D	-17.5	10.7	394.4	-19.5	528.1	415.9
ELIMINATE D	-6.8	4.9	27.3	-32.2	24.5	10.1
MICROSTRAIN/ UNIT VxD	-0.19×10^{-5}	0.14×10^{-5}	0.76×10^{-5}	-0.90×10^{-5}	0.68×10^{-5}	0.28×10^{-5}

TABLE B20

LOAD	$V=3628.8$ kgf; $M_D=-0.183V$ kgf.m; $D=1307.1$ kgf; $\delta=0.0848$m; $S=M_V=M_S=0$					
RUN	ε_1	ε_2	ε_3	ε_4	ε_5	ε_6
1	-1012.0	1193.0	315.0	89.0	428.0	440.0
ELIMINATE V AND M_D	-8.6	4.6	362.2	15.0	458.3	405.2
ELIMINATE $V\times\delta$	-8.6	4.6	362.2	-1.4	460.8	405.2
ELIMINATE D	2.0	-1.2	-1.9	-14.0	-38.7	2.7
ELIMINATE VxD				28.7	-70.9	
MICROSTRAIN/ UNIT VxD	0.04×10^{-5}	-0.02×10^{-5}	-0.04×10^{-5}			0.06×10^{-5}
MICROSTRAIN/ UNIT $D\times\delta$				0.259	-0.640	

TABLE B21

k^+_{m2V}	k^+_{12V}	k^+_{22V}	k^+_{32V}	k^+_{42V}	k^+_{52V}	k^+_{62V}
MICROSTRAIN/ UNIT VxD	-0.07×10^{-5}	0.06×10^{-5}	0.36×10^{-5}	-0.90×10^{-5}	0.68×10^{-5}	0.17×10^{-5}

Tests of negative drag load combined with vertical load were not performed on the port leg and so Tables B22 to B24 do not exist and Table B25 lists the positive load parameter values to apply for both positive and negative loading.

TABLE B25

k_{12V}	k_{22V}	k_{32V}	k_{42V}	k_{52V}	k_{62V}	$k_{42\delta}$	$k_{52\delta}$
-0.07×10^{-5}	0.06×10^{-5}	0.36×10^{-5}	-0.90×10^{-5}	0.68×10^{-5}	0.17×10^{-5}	0.259	-0.640

DISTRIBUTION

	COPY NO.
AUSTRALIA	
Department of Defence	
Central Office	
Chief Defence Scientist	1
Deputy Chief Defence Scientist	2
Superintendent, Science and Technology Programs	3
Defence Library	4
Assistant Secretary, D.I.S.B.	5-20
Joint Intelligence Organisation	21
Aust. Defence Science and Technical Representative (UK)	22
Counsellor, Defence Science (USA)	23
Aeronautical Research Laboratories	
Chief Superintendent	24
Library	25
Superintendent Division - Structures	26
Divisional File - Structures	27
Authors: K.C. Watters	28
P. Rtcliffe	29
B.C. Hoskin	30
Materials Research Laboratories	
Library	31
Defence Research Laboratories, Salisbury	
Library	32
Air Force Office	
Aircraft Research and Development Unit	33
Statutory, State Authorities and Industry	
Commonwealth Aircraft Corporation (Library)	34
SPARES	35-44